

# Synthesis, ligand–receptor modeling studies and pharmacological evaluation of novel 4-modified-2-aryl-1,2,4-triazolo[4,3-*a*]quinoxalin-1-one derivatives as potent and selective human A<sub>3</sub> adenosine receptor antagonists

Vittoria Colotta,<sup>a,\*</sup> Daniela Catarzi,<sup>a</sup> Flavia Varano,<sup>a</sup> Ombretta Lenzi,<sup>a</sup> Guido Filacchioni,<sup>a</sup> Claudia Martini,<sup>b</sup> Letizia Trincavelli,<sup>b</sup> Osele Ciampi,<sup>b</sup> Chiara Traini,<sup>c</sup> Anna Maria Pugliese,<sup>c</sup> Felicita Pedata,<sup>c</sup> Erika Morizzo<sup>d</sup> and Stefano Moro<sup>d</sup>

<sup>a</sup>*Dipartimento di Scienze Farmaceutiche, Laboratorio di Progettazione, Sintesi e Studio di Eterocicli Biologicamente Attivi, Università di Firenze, Polo Scientifico, Via Ugo Schiff, 6, 50019 Sesto Fiorentino, FI, Italy*

<sup>b</sup>*Dipartimento di Psichiatria, Neurobiologia, Farmacologia e Biotecnologie, Via Bonanno, 6, 56126 Pisa, Italy*

<sup>c</sup>*Dipartimento di Farmacologia Preclinica e Clinica, Università di Firenze, Viale Pieraccini 6, 50139 Firenze, Italy*

<sup>d</sup>*Molecular Modeling Section, Dipartimento di Scienze Farmaceutiche, Università di Padova, via Marzolo 5, 35131 Padova, Italy*

Received 9 January 2008; revised 9 April 2008; accepted 18 April 2008

Available online 24 April 2008

**Abstract**—The study of some 4-substituted-2-aryl-1,2,4-triazolo[4,3-*a*]quinoxalin-1-one derivatives, designed as hA<sub>3</sub> adenosine receptor antagonists, is reported. The new compounds bear on the four-position different acylamino, sulfonylamino, benzylureido and benzyloxy moieties, which have also been combined with a *para*-methoxy group on the 2-phenyl ring or with a nitro residue at the six-position. Many derivatives show high hA<sub>3</sub> adenosine receptor affinities and selectivities both versus hA<sub>1</sub> and hA<sub>2A</sub> receptors. The observed structure–affinity relationships of this class of antagonists have been exhaustively rationalized using the recently published ligand-based homology modeling (LBHM) approach. The selected 4-bismethanesulfonylamino-2-phenyl-1,2,4-triazolo[4,3-*a*]quinoxalin-1-one (**13**), which shows high hA<sub>3</sub> affinity ( $K_i = 5.5$  nM) and selectivity versus hA<sub>1</sub>, hA<sub>2A</sub> (both selectivity ratios > 1800) and hA<sub>2B</sub> (cAMP assay, IC<sub>50</sub> > 10,000 nM) receptors, was tested in an *in vitro* rat model of cerebral ischemia, proving to be effective in preventing the failure of synaptic activity, induced by oxygen and glucose deprivation in the hippocampus, and in delaying the occurrence of anoxic depolarization.

© 2008 Elsevier Ltd. All rights reserved.

## 1. Introduction

The modulator adenosine plays important roles in a wide variety of physiological functions, both in the central nervous system and in the periphery. Adenosine exerts its effects through activation of four cell membrane receptors, termed A<sub>1</sub>, A<sub>2A</sub>, A<sub>2B</sub>, and A<sub>3</sub>, which belong to the super family of G protein-coupled receptors.<sup>1,2</sup> Activation of adenosine receptors (ARs) modulates adenylyl cyclase activity, either in a negative (A<sub>1</sub> and A<sub>3</sub>) or po-

sitive manner (A<sub>2A</sub> and A<sub>2B</sub>)<sup>1</sup> but it can also modulate other intracellular signaling pathways. In particular, the A<sub>3</sub> receptor subtype is positively coupled to phospholipase C<sup>3</sup> and D,<sup>4</sup> K<sub>ATP</sub> channels<sup>5</sup> and it was also proven to induce calcium mobilization.<sup>5</sup> The A<sub>3</sub> AR is widely distributed in mammals, and in humans it is highly expressed in lung and liver, with lower levels in aorta, brain, and testes.<sup>6</sup> The growing understanding of the physiological effects mediated by the A<sub>3</sub> subtype, such as modulation of cerebral and cardiac ischemia,<sup>6,7</sup> inflammation,<sup>8</sup> or normal and tumor cell regulation,<sup>9</sup> makes this receptor subtype an interesting target for various therapeutic interventions.<sup>10</sup> A<sub>3</sub> AR antagonists are being investigated as potential agents in renal injury,<sup>11</sup> neuroprotective agents<sup>12,13</sup> and, recently, they have been described as potential therapeutics in the treatment of glioblastoma multiforme.<sup>14</sup>

**Keywords:** G protein-coupled receptors; Adenosine receptor antagonists; Triazolo[4,3-*a*]quinoxalin-1-ones; Tricyclic heteroaromatic systems; Ligand–receptor modeling studies; Neuroprotective agents.

\* Corresponding author. Tel.: +39 55 5253731; fax: +39 55 5253780; e-mail: [vittoria.colotta@unifi.it](mailto:vittoria.colotta@unifi.it)

In the past few years, we have directed some of our research toward the study of AR antagonists belonging to different tricyclic systems.<sup>15–23</sup> Among them, the 2-aryl-1,2,4-triazolo[4,3-*a*]quinoxalin-1-one derivatives were widely investigated by probing different substituents on the 2-phenyl moiety, the fused benzo ring, and the four-position (Chart 1). These studies led to the identification of some structural elements which shift the affinity toward the human A<sub>3</sub> (hA<sub>3</sub>) receptor subtype. The crucial groups which afforded nanomolar affinity and high selectivity were a 4-methoxy group on the 2-phenyl ring,<sup>16</sup> acyl moieties on the 4-amino group,<sup>16</sup> or a 6-nitro substituent on the fused benzo ring.<sup>17</sup> Interestingly, hindering substituents on the 4-amino group were also well tolerated.<sup>22</sup> The contemporary functionalization of the 2-phenyl-1,2,4-triazolo[4,3-*a*]quinoxalin-1-one scaffold with the above cited substituents generally maintained high hA<sub>3</sub> AR affinity and selectivity.<sup>22</sup> Molecular modeling studies were carried out to rationalize the observed structure–affinity relationships (SAR) and to recognize the hypothetical binding motif of these compounds in our rhodopsin-based homology model of human A<sub>3</sub> AR. Several hydrogen-bonding interactions seem to stabilize the anchoring of the ligands inside the binding cleft.<sup>19,20,22</sup> These bonds involve the 1-carbonyl group, the 6-nitro substituent, and the 4-acylamino chain, at the level of both NH and CO functions.<sup>20,22</sup> Interestingly, the two hydrogen bonds of the 4-NH–CO moiety appropriately orient the R residue inside a hydrophobic pocket. Also the 2-aryl and the fused benzo ring are located in two size-limited pockets. Obviously, although most of the previously investigated triazoloquinoxalin-1-one derivatives share a similar binding mode inside the transmembrane region (TM) of the hA<sub>3</sub> receptor, each compound finds a fine adjustment in the receptor cavity to optimize the electrostatic and steric interactions depending on the nature of the substituents on the triazoloquinoxalin-1-one scaffold. In this context, the substituent on the 4-amino group seems to play a critical role. On this basis, we syn-

thesized a new series of 1,2,4 triazolo[4,3-*a*]quinoxalin-1-one derivatives (Chart 1 and Table 1), bearing on the 4-amino group some acyl, sulfonyl, and carbamoyl residues, which were also combined with a methoxy substituent or a nitro group at the R<sub>1</sub> and R<sub>6</sub> positions, respectively (compounds 1–19). The 4-benzyloxy derivatives 20–21 were also prepared with the purpose of evaluating whether the 4-NHCO-group was essential for the anchoring at the hA<sub>3</sub> receptor site. Molecular modeling studies were carried out on the new derivatives in order to rationalize their hA<sub>3</sub> affinity data and describe their putative binding mode in our model of the hA<sub>3</sub>AR recognition site. Moreover, a selected compound, the 4-bis-methanesulfonylamino-2-phenyl derivative 13, was tested in an in vitro rat model of cerebral ischemia to assess its effect in the failure of synaptic activity induced by oxygen and glucose deprivation.

## 2. Chemistry

The target derivatives 1–21 (Chart 1 and Table 1) were prepared as depicted in Schemes 1–4.

Synthesis of the 2-aryl-1,2,4-triazolo[4,3-*a*]quinoxalin-1-one derivatives 1–3 and 4–6, bearing, respectively, 4-arylamino moieties or the 4-pyridylcarbonylamino group, was performed by reacting the suitable 4-amino-triazoloquinoxalines 22,<sup>16</sup> 23,<sup>16</sup> or 24<sup>17</sup> with the corresponding acyl chlorides in anhydrous dichloromethane or pyridine (Scheme 1). The 4-sulfonylamino-triazoloquinoxaline derivatives 7–12 were obtained allowing the 4-amino-triazoloquinoxaline derivatives 22–24 to react with the suitable sulfonyl chlorides (Scheme 2). The 4-bis-methanesulfonylamino-derivatives 13–14 were synthesized by reacting 22 and 24 with an excess of methanesulfonylchloride (Scheme 2). The 4-ureido-triazoloquinoxaline derivatives 15–19 were obtained when compounds 22–24 were refluxed with different isocyanates in anhydrous tetrahydrofuran (Scheme 3). The

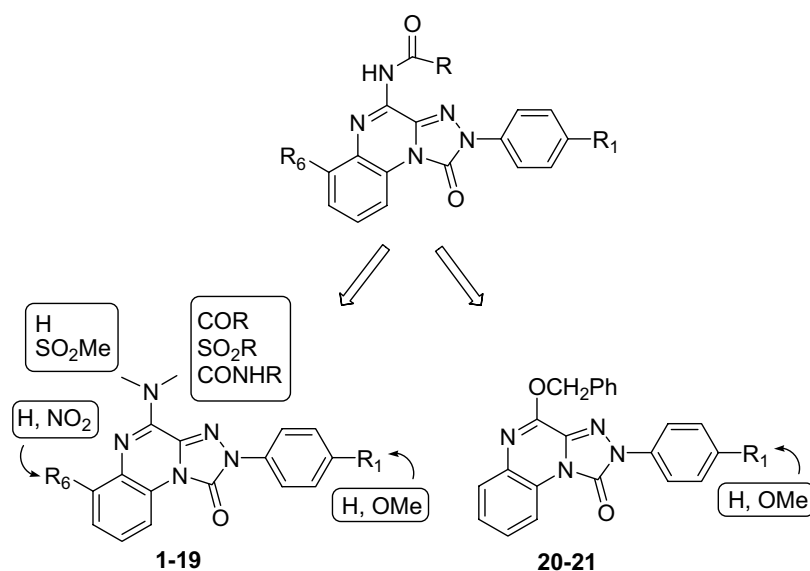
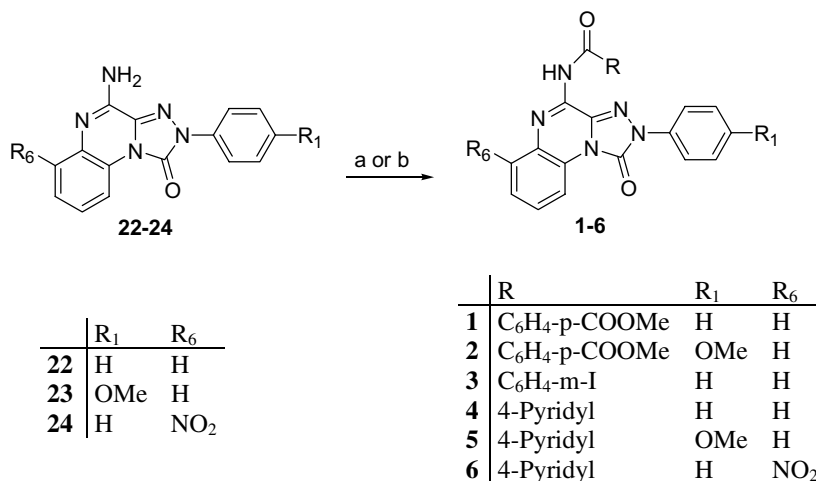
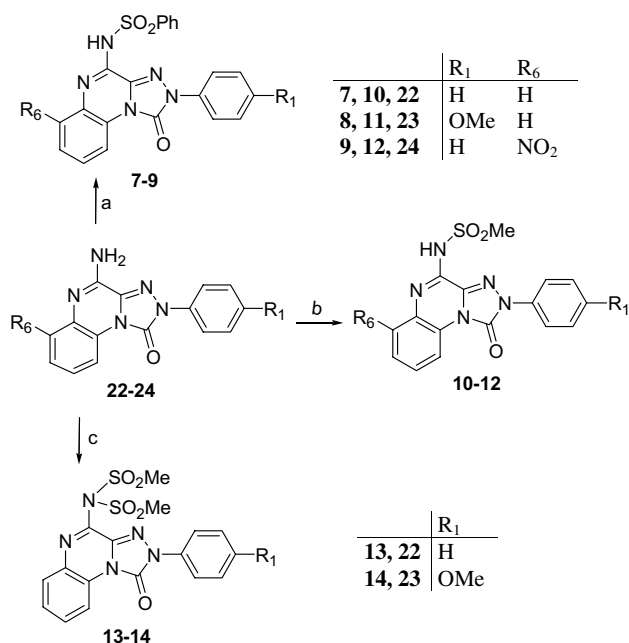


**Chart 1.** Previously and herein-reported 4-modified 2-aryl-1,2,4-triazolo[4,3-*a*]quinoxalin-1-one derivatives.



**Scheme 1.** Reagents and conditions: (a) RCOCl, anhydrous pyridine, reflux 10–20 h, 80–97%; (b) RCOCl, anhydrous CH<sub>2</sub>Cl<sub>2</sub> and pyridine, reflux 3 h, 79%.



**Scheme 2.** Reagents and conditions: (a) PhSO<sub>2</sub>Cl, anhydrous CH<sub>2</sub>Cl<sub>2</sub> and/or pyridine, reflux 36–140 h, 64–77%; (b) MeSO<sub>2</sub>Cl, anhydrous CH<sub>2</sub>Cl<sub>2</sub> and/or pyridine, reflux 14–72 h, 30–50%; (c) excess of MeSO<sub>2</sub>Cl, anhydrous CH<sub>2</sub>Cl<sub>2</sub> and pyridine, reflux 15–38 h, 60–85%.

4-benzyloxy-triazoloquinoxalin-1-one derivatives **20–21** were prepared from the corresponding 4-chloro derivatives **25–26**<sup>16</sup> and benzyl alcohol, in the presence of sodium hydride in dimethylsulfoxide (Scheme 4).

### 3. Pharmacology

Compounds **1–21** were tested for their ability to displace [<sup>3</sup>H]8-cyclopentyl-1,3-dipropylxanthine ([<sup>3</sup>H]DPCPX) from A<sub>1</sub> AR in bovine cerebral cortical membranes, [<sup>3</sup>H]2-[4-(2-carboxyethyl)phenethyl]amino-5'-(*N*-ethyl-carbamoyl)adenosine ([<sup>3</sup>H]CGS 21680) from A<sub>2A</sub> AR in bovine striatal membranes, and [<sup>125</sup>I]N<sup>6</sup>-(4-amino-3-iodo-

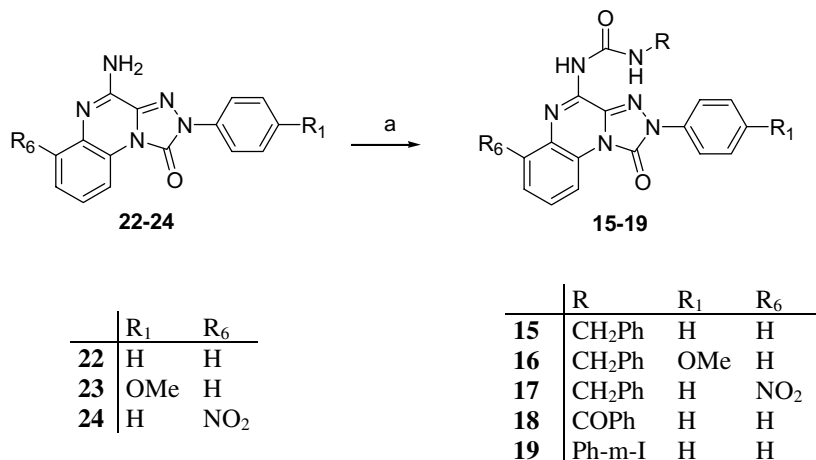
obenzyl)-5'-(*N*-methylcarbamoyl)adenosine ([<sup>125</sup>I]AB-MECA) from cloned hA<sub>3</sub> receptor stably expressed in CHO cells. Subsequently, the selected compounds **4–5**, **7–8**, **13**, **15–17**, and **20–21**, which showed high to good hA<sub>3</sub> AR affinity (*K<sub>i</sub>* < 100 nM), were tested for their ability to displace [<sup>3</sup>H]DPCPX from cloned hA<sub>1</sub> AR and [<sup>3</sup>H]5'-(*N*-ethyl-carboxamido)adenosine ([<sup>3</sup>H]NECA) from cloned hA<sub>2A</sub> ARs, in order to establish their A<sub>3</sub> versus A<sub>1</sub> and A<sub>3</sub> versus A<sub>2A</sub> selectivity within the same species. The binding data of **1–21** are shown in Table 1, together with those of the 4-benzoylamino-1,2-dihydro-2-phenyl-1,2,4-triazolo[4,3-*a*]quinoxalin-1-one **A**,<sup>22</sup> theophylline, and DPCPX, reported as comparison. The 4-bismethanesulfonylamino derivative **13**, which showed one of the highest hA<sub>3</sub> receptor affinities and selectivities versus hA<sub>1</sub> and hA<sub>2A</sub> subtypes, among the herein reported compounds, was selected for evaluating: (a) its potency toward the hA<sub>3</sub> receptor by determining the inhibitory effect on NECA-inhibited cAMP production in hA<sub>3</sub> transfected CHO cells; (b) its affinity and selectivity toward the hA<sub>2B</sub> receptor by evaluating its effect on NECA-stimulated cAMP levels in hA<sub>2B</sub> transfected CHO cells.

Derivative **13** was also tested to assess its affinity at rat (r) A<sub>1</sub> and A<sub>3</sub> ARs. The rA<sub>1</sub> affinity was evaluated by competition experiments using [<sup>3</sup>H]DPCPX in rat cerebral cortex and the rA<sub>3</sub> affinity was determined using [<sup>3</sup>H](R)-PIA in rat testis membranes, in the presence of DPCPX to block A<sub>1</sub> binding sites. Finally, compound **13** was tested in electrophysiological experiments in rat hippocampus to evaluate its efficacy in delaying the irreversible failure of synaptic activity induced by oxygen and glucose deprivation.

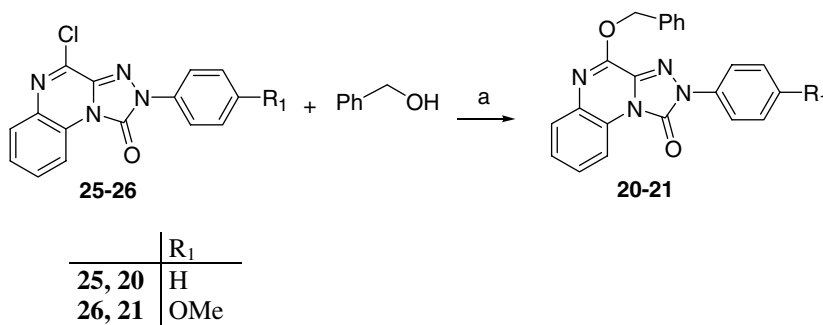
## 4. Results and discussion

### 4.1. Structure–affinity relationships

The binding results reported in Table 1 indicate that some of the newly synthesized 1,2,4-triazolo[4,3-*a*]qui-



**Scheme 3.** Reagents and conditions: (a) R-N=C=O, anhydrous tetrahydrofuran, reflux 3–36 h, 55–95%.



**Scheme 4.** Reagents and conditions: (a) 60% NaH dispersion in mineral oil, anhydrous dimethylsulfoxide, rt 12–15 h, 35–48%.

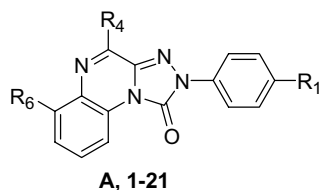
noxalin-1-ones show high hA<sub>3</sub> receptor affinity and selectivity (compounds **7–8**, **13**, **16**, **17**, and **20–21**) both versus hA<sub>1</sub> and hA<sub>2A</sub> ARs.

Considering the previously reported 4-benzoylamino-1,2-dihydro-2-phenyl-1,2,4-triazolo[4,3-*a*]quinoxalin-1-one **A**<sup>22</sup> as reference compound, we can observe that introduction of a *para*-carbomethoxy group or a *meta*-iodo substituent on the benzoyl moiety was deleterious for the hA<sub>3</sub> receptor affinity (compounds **1** and **3**), probably because of the steric bulk enhancement of the 4-arylamino portion. The same negative effect was produced on affinities at all the other investigated receptors. Isosteric replacement of the benzoyl residue of **A** with a 4-pyridylcarbonyl moiety (compound **4**) maintained the hA<sub>3</sub> affinity in the low nanomolar range and decreased the capability to bind the hA<sub>1</sub> receptor, thus enhancing the hA<sub>3</sub> versus hA<sub>1</sub> selectivity. Compound **4** also displays some (30-fold) hA<sub>3</sub> versus hA<sub>2A</sub> receptor selectivity. Replacement of the 4-benzoylamino group of **A** with the 4-benzenesulfonylamino moiety (compound **7**) was made because we hypothesized that the sulfonyl group could engage a hydrogen bond with the receptor site, similarly to the benzoyl carbonyl group of compound **A**. This structural modification, although affording some reduction of the hA<sub>3</sub> AR affinity ( $K_i = 32$  nM), significantly increased the selectivity for the hA<sub>3</sub> receptor subtype, being both hA<sub>1</sub> and hA<sub>2A</sub> receptor affinities null. Replacement of the 4-benzenesulfonylamino moiety of

compound **7** with a 4-methanesulfonylamino chain (compound **10**) dramatically decreased the hA<sub>3</sub> AR affinity ( $K_i = 1427$  nM), probably because of the reduction of the lipophilicity of the substituent and, consequently, of the weaker hydrophobic interaction of compound **10** with the receptor site. When a second methanesulfonyl group was introduced on the 4-amino moiety of **10**, the hA<sub>3</sub> affinity significantly ameliorated. Indeed, compound **13** binds the hA<sub>3</sub> subtype with nanomolar affinity ( $K_i = 5.5$  nM) and also with high selectivity, versus both hA<sub>1</sub> and hA<sub>2A</sub> receptors. To determine also its hA<sub>3</sub> versus hA<sub>2B</sub> selectivity, we tested compound **13** in cAMP assays, which evidenced a lack of hA<sub>2B</sub> affinity, being **13** ineffective in inhibiting NECA-stimulated cAMP levels in hA<sub>2B</sub> CHO cells ( $IC_{50} > 10,000$ ).

Among the probed ureido substituents (compound **15–19**) only the benzylureido chain afforded a significant hA<sub>3</sub> affinity (compounds **15–17**). A very interesting result was found for the 4-benzyloxy derivative **20**, which possesses a high affinity for the hA<sub>3</sub> AR ( $K_i = 21$  nM), although lacking the 4-NH-CO- group. This derivative is also highly hA<sub>3</sub> selective, in comparison to both the hA<sub>1</sub> and hA<sub>2A</sub>.

The *para*-methoxy substituent at the R<sub>1</sub> position was beneficial in compounds **2**, **8**, **11**, and **21** since they show higher hA<sub>3</sub> AR affinities with respect to the corresponding 2-phenyl derivatives **1**, **7**, **10**, and **20**. In the other

**Table 1.** Binding affinity at human A<sub>1</sub>, A<sub>2A</sub>, A<sub>3</sub> and bovine A<sub>1</sub>, and A<sub>2A</sub> ARs

Compound	R <sub>4</sub>	R <sub>1</sub>	R <sub>6</sub>	K <sub>i</sub> <sup>a</sup> (nM) or I/%				
				hA <sub>3</sub> <sup>b</sup>	hA <sub>1</sub> <sup>c</sup>	hA <sub>2A</sub> <sup>d</sup>	bA <sub>1</sub> <sup>e</sup>	bA <sub>2A</sub> <sup>f</sup>
A <sup>g</sup>	NHCOPh	H	H	1.47 ± 0.06	87.8 ± 6.3	88.2 ± 6.7	89.6 ± 7.2	53%
<b>1</b>	NHCOC <sub>6</sub> H <sub>4</sub> -4COOMe	H	H	41%			106 ± 2.1	36%
<b>2</b>	NHCOC <sub>6</sub> H <sub>4</sub> -4COOMe	OMe	H	1370 ± 121			30.5%	41%
<b>3</b>	NHCOC <sub>6</sub> H <sub>4</sub> -3I	H	H	36%			473 ± 34	35%
<b>4</b>	NHCO-4-Pyridyl	H	H	6.1 ± 0.5	2379 ± 191	188 ± 9.4	57 ± 4.3	812 ± 71
<b>5</b>	NHCO-4-Pyridyl	OMe	H	68 ± 5.2	779 ± 53	397 ± 39	236 ± 15	44%
<b>6</b>	NHCO-4-Pyridyl	H	NO <sub>2</sub>	0%			37.5%	22%
<b>7</b>	NHSO <sub>2</sub> Ph	H	H	32.2 ± 2.8	0%	27%	157 ± 1.4	35%
<b>8</b>	NHSO <sub>2</sub> Ph	OMe	H	2.2 ± 0.11	2700 ± 142	23%	4700 ± 260	16%
<b>9</b>	NHSO <sub>2</sub> Ph	H	NO <sub>2</sub>	100 ± 7.2			210 ± 12	25%
<b>10</b>	NHSO <sub>2</sub> CH <sub>3</sub>	H	H	1427 ± 125			164 ± 11.3	32%
<b>11</b>	NHSO <sub>2</sub> CH <sub>3</sub>	OMe	H	493 ± 33			6%	0%
<b>12</b>	NHSO <sub>2</sub> CH <sub>3</sub>	H	NO <sub>2</sub>	37%			2840 ± 162	25%
<b>13</b>	N(SO <sub>2</sub> CH <sub>3</sub> ) <sub>2</sub>	H	H	5.5 ± 0.4	36%	32%	36 ± 1.3	56%
<b>14</b>	N(SO <sub>2</sub> CH <sub>3</sub> ) <sub>2</sub>	OMe	H	387 ± 24			6.2%	17%
<b>15</b>	NHCONHCH <sub>2</sub> Ph	H	H	83.5 ± 4.9	12.3 ± 1.2	158.3 ± 15	4.1 ± 0.2	172.6 ± 12
<b>16</b>	NHCONHCH <sub>2</sub> Ph	OMe	H	65 ± 5.1	4215 ± 350	23%	20.8 ± 1.2	12%
<b>17</b>	NHCONHCH <sub>2</sub> Ph	H	NO <sub>2</sub>	63 ± 4.4	4%	20%	4.6 ± 0.3	46.5%
<b>18</b>	NHCONHCOPh	H	H	1300 ± 115			100.6 ± 8.9	379 ± 24
<b>19</b>	NHCONH-Ph-3I	H	H	953 ± 61			359 ± 25	1800 ± 150
<b>20</b>	OCH <sub>2</sub> Ph	H	H	21 ± 1.8	46%	10%	55 ± 3.6	19%
<b>21</b>	OCH <sub>2</sub> Ph	OMe	H	6.4 ± 0.4	54%	4%	53 %	41%
Theophylline				86,000 ± 7800	6200 ± 530	7900 ± 630	3800 ± 340	21,000 ± 1800
DPCPX				1300 ± 125	3.2 ± 0.2	260 ± 18	0.5 ± 0.03	337 ± 28

<sup>a</sup> The K<sub>i</sub> values are means ± SEM of four separate assays, each performed in triplicate.

<sup>b</sup> Displacement of specific [<sup>125</sup>I]AB-MECA binding at hA<sub>3</sub> receptors expressed in CHO cells or percentage of inhibition (I%) of specific binding at 1 μM concentration.

<sup>c</sup> Displacement of specific [<sup>3</sup>H]DPCPX binding at hA<sub>1</sub> receptors expressed in CHO cells or percentage of inhibition (I%) of specific binding at 10 μM concentration.

<sup>d</sup> Displacement of specific [<sup>3</sup>H]NECA binding at hA<sub>2A</sub> receptors expressed in CHO cells or percentage of inhibition (I%) of specific binding at 10 μM concentration.

<sup>e</sup> Displacement of specific [<sup>3</sup>H]DPCPX binding in bovine brain membranes or percentage of inhibition (I%) of specific binding at 10 μM concentration.

<sup>f</sup> Displacement of specific [<sup>3</sup>H]CGS 21680 binding from bovine striatal membranes or percentage of inhibition (I%) of specific binding at 10 μM concentration.

<sup>g</sup> Ref. 22.

cases, the *para*-methoxy group left almost unchanged (compare compound **16** with **15**) or worsened (compare compounds **5** and **14** with **4** and **13**, respectively) the binding at the hA<sub>3</sub> receptor.

Introduction of the nitro group at the R<sub>6</sub> position was not beneficial as it reduced the hA<sub>3</sub> affinity (compare **7** with **9** and **10** with **12**) or annulled it (compare **4** with **6**). The only exception is represented by the 4-benzylureido derivative **17**, which possesses the same good hA<sub>3</sub> AR affinity of the 6-unsubstituted parent derivative **15**, and also higher hA<sub>3</sub> receptor selectivity.

The selected 4-bismethanesulfonylamino derivative **13** was tested to assess its potency versus the hA<sub>3</sub> receptor. Consistently with its high hA<sub>3</sub> affinity value (K<sub>i</sub> = 5.5 nM), compound **13** proved to be highly potent

in inhibiting the NECA-inhibited cAMP accumulation in hA<sub>3</sub> CHO cells showing an antagonistic behaviour (Fig. 1, EC<sub>50</sub> = 12 ± 1.1 nM). Since compound **13** was tested in an in vitro rat model of cerebral ischemia, we also evaluated its rA<sub>1</sub> and rA<sub>3</sub> AR affinities. As expected, the rat A<sub>3</sub> affinity was very low. At 1 μM concentration, it inhibited the radioligand-binding by only 5%. On the contrary, the ability of compound **13** to displace rA<sub>1</sub> ligand from its receptor was significantly higher (K<sub>i</sub> = 132 ± 12 nM) than shown for hA<sub>1</sub> receptor.

The bA<sub>1</sub> and bA<sub>2A</sub> binding data of the new derivatives **1–21** (Table 1) warrant some comments. As expected, none of the compounds significantly bind to the bA<sub>2A</sub> AR, with the exception of three derivatives (**4**, **15**, and **18**). In contrast, several derivatives (**1**, **4**, **13**, **15**, and **18–20**), all lacking both the R<sub>1</sub> and R<sub>6</sub> substituents, pos-

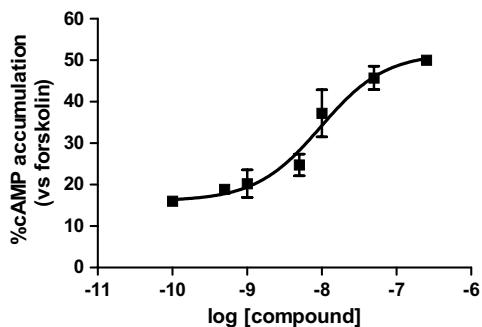


**Figure 1.** Effect of compound **13** on NECA-mediated cAMP accumulation (vs forskolin, set to 100%) in CHO cells stably expressing hA<sub>3</sub> AR. Data represents means  $\pm$  SEM from three separate experiments. The IC<sub>50</sub> value for **13** was  $12 \pm 1.2$  nM.

sess high to good bA<sub>1</sub> affinities. As previously observed in this class of AR antagonists,<sup>16,19,22</sup> the methoxy group at the R<sub>1</sub> position decreases the binding at the bA<sub>1</sub> receptor. Indeed, all the 2-(4-methoxyphenyl)-derivatives (**2**, **5**, **8**, **11**, **14**, **16**, and **21**) show lower bA<sub>1</sub> receptor affinities than those of the corresponding 2-phenyl-substituted compounds (**1**, **4**, **7**, **10**, **13**, **15**, and **20**). Instead, the nitro group at the R<sub>6</sub> position does not exert a constant effect: derivatives **6** and **12** show significantly reduced bA<sub>1</sub> affinities, in comparison to their 6-des nitro compounds **4** and **10**, while compounds **9** and **17** display similar bA<sub>1</sub> AR affinities to those of derivatives **7** and **15**.

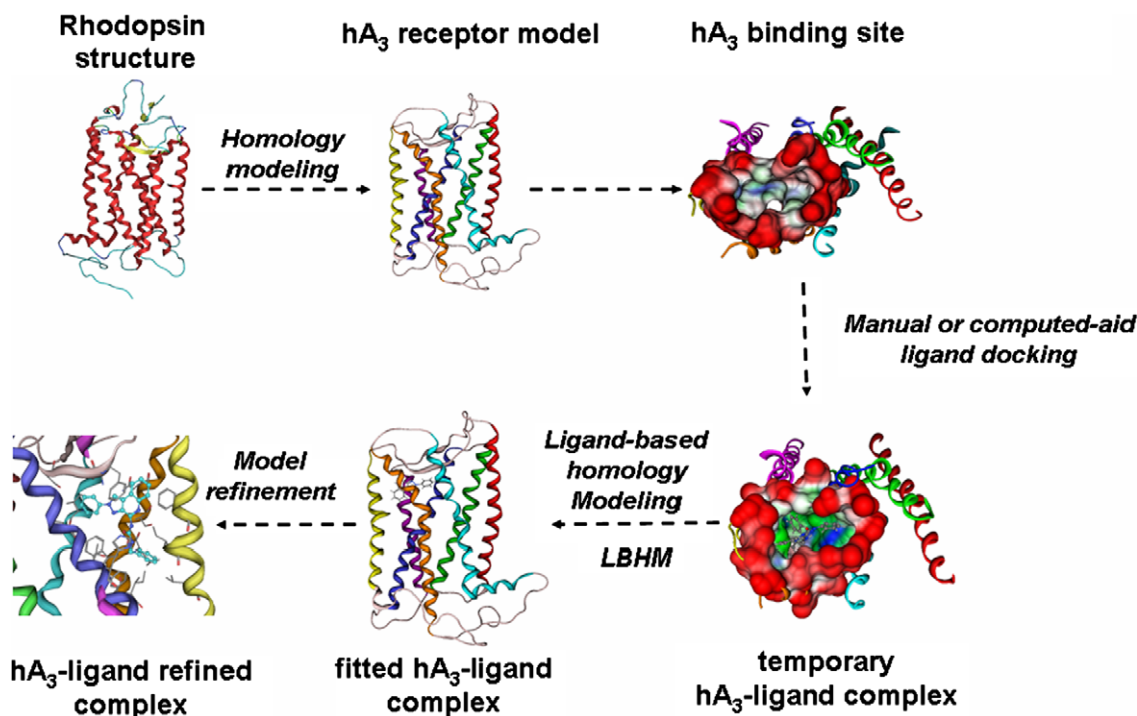
It is worth noting that these compounds show significantly different affinities at the bA<sub>1</sub> receptor than at

the hA<sub>1</sub> one, in perfect accordance with the results obtained in previous studies, either on this<sup>19,22</sup> or other classes of derivatives.<sup>20,21,23–26</sup> These results confirm that, notwithstanding the high sequence homology (94%) between the human and bovine A<sub>1</sub> receptors,<sup>24</sup> significant structural differences exist in the region of the recognition site of the two receptors.

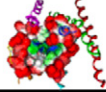
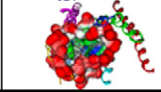
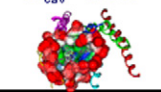
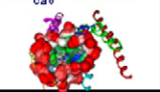
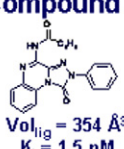
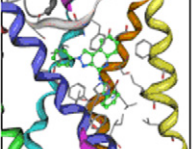
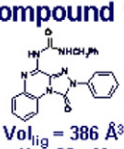
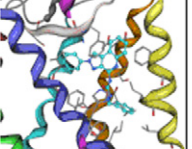
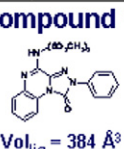
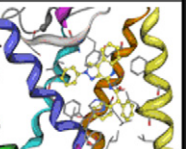
## 4.2. Molecular modeling studies

Molecular modeling studies were performed on the 2-aryl-1,2,4-triazolo[4,3-*a*]quinoxalin-1-one derivatives **A** and **1–21** in order to identify the hypothetical binding motif of the new hA<sub>3</sub> antagonists and rationalize the observed SAR.

Following our previously reported modeling studies,<sup>19–23</sup> we have constructed a refined model of hA<sub>3</sub> receptor by using a rhodopsin-based homology modeling (RBHM) approach.<sup>27–30</sup> Moreover, our recently described ligand-based homology modeling (LBHM) approach has been used to simulate the conformational changes induced by ligand binding, and a schematic representation of the ligand-based homology protocol is shown in Figure 2 (methodological details are summarized in Section 6.2).<sup>31</sup> As reported in Figure 3, depending on the topological properties of the different ligands, we found four different conformational models of the human A<sub>3</sub> receptor reverse agonist-like state in which both shape and chemical complementarities have been specifically optimized around each ligand. In this specific case, with varying ligand structure, the molecular volume of the transmembrane (TM) binding cavity changes from the 660 Å<sup>3</sup> of the standard RBHM-driven



**Figure 2.** Flow chart of the ligand-based homology modeling (LBHM) technique considering an evolution of a conventional rhodopsin-based homology modeling (RBHM) algorithm.

Reference derivative	Docked derivatives	Rhodopsin-based homology model Vol <sub>cav</sub> = 660 Å <sup>3</sup> 	LBHM: model 1 (using compound A as reference structure) Vol <sub>cav</sub> = 910 Å <sup>3</sup> 	LBHM: model 2 (using compound 15 as reference structure) Vol <sub>cav</sub> = 980 Å <sup>3</sup> 	LBHM: model 3 (using compound 13 as reference structure) Vol <sub>cav</sub> = 1120 Å <sup>3</sup> 
<b>Compound A</b>  Vol <sub>lig</sub> = 354 Å <sup>3</sup> K <sub>i</sub> = 1.5 nM	 <b>compounds 1–12, 20–21</b>	NO REASONABLE DOCKING POSES			
<b>Compound 15</b>  Vol <sub>lig</sub> = 386 Å <sup>3</sup> K <sub>i</sub> = 83 nM	 <b>compounds 16–19</b>	NO REASONABLE DOCKING POSES	NO REASONABLE DOCKING POSES		
<b>Compound 13</b>  Vol <sub>lig</sub> = 384 Å <sup>3</sup> K <sub>i</sub> = 5.5 nM	 <b>compounds 13–14</b>	NO REASONABLE DOCKING POSES	NO REASONABLE DOCKING POSES	NO REASONABLE DOCKING POSES	

**Figure 3.** Ligand-based homology modeling (LBHM) data collection. Each ‘reference derivative’ (compounds A, 13 and 15) was used as ligand-template during the homology modeling process. Consequently, four different conformational states (models 1–4) were selected as putative ambassadors of the conformational changes induced by different ligand binding. Depending on their different structure topologies, all other antagonists (docked derivatives) were docked into the most complementary receptor models.

model to the 1120 Å<sup>3</sup> of the largest LBHM-driven model, without altering the conventional rhodopsin-like receptor topology. The modifications of both shape and volume of the human A<sub>3</sub> TM binding cavity are the most important receptor modeling perturbations obtained by the application of the LBHM technique. The binding cavity reorganization induced by ligand binding is due to the conformational change in several amino acid side chains, such as Leu90 (3.32), Leu91 (3.33), Thr94 (3.36), His95 (3.37), Ile98 (3.40), Gln167 (EL2), Phe168 (EL2), Phe182 (5.43), Ile186 (5.47), Leu190 (5.51), Phe239 (6.44), Trp243 (6.48), Leu244 (6.49), Leu264 (7.35), and Ile268 (7.39). However, molecular docking studies carried out for all the triazoloquinoxaline antagonists, using the appropriate conformational states of the receptor as listed in Figure 3, have shown a similar binding motif indicating that a common receptor-driven pharmacophore model can be depicted. This finding is coherent with our previously reported studies.<sup>23,27–31</sup> Interestingly, none of the new triazoloquinoxaline antagonists found an energetically stable docking pose in the conventional RBHM-driven A<sub>3</sub> model. This is mainly due to the unfavorable topological complementarity among these antagonists and corresponding RBHM-driven TM binding cavity. In particular, highly destabilizing van der Waals interactions (steric conflicts) seem to be the reason for lacking topological complementarities. These steric conflicts are drastically reduced or completely eliminated after the application of the LBHM approach.

As previously described,<sup>19–22</sup> ligand recognition occurs in the upper region of the TM bundle, and the triazolo-

quinoxaline moiety is surrounded by TMs 3, 5, 6, and 7 with the substituent in the four-position oriented toward the intracellular environment. Furthermore, this hypothetical binding cleft has also been recently hypothesized by other authors.<sup>32,33</sup> As shown in Figure 4, the phenyl ring at the two-position is close to TMs 3, 6, and 7. Analyzing our model in detail, all triazoloquinoxaline derivatives share at least two stabilizing hydrogen-bonding interactions inside the binding cleft. The first hydrogen bond is between the carbonyl group at one-position, that points toward the EL2, and the NH<sub>2</sub> of the Gln167. This hydrogen-bonding distance is calculated around 2.8 Å for all docked compounds. Moreover, the 1-carbonyl group is also at the hydrogen-bonding distance (ca. 3.2 Å) with the amide moiety of Asn250 (6.55) side chain. This asparagine residue, conserved among all adenosine receptor subtypes, was found to be important for ligand binding.<sup>34,35</sup>

An important hydrogen-bonding network can be observed in all energetically stable docked conformations of all the triazoloquinoxaline antagonists; in particular, Thr94 (3.36), His95 (3.37), and Ser247 (6.52) are able to interact through hydrogen bonds with the 4-carbonyl oxygen of compounds 1–19 and with the ether oxygen of derivatives 20–21. These polar amino acids seem to be critical for the recognition of all antagonist structures and for receptor selectivity. In particular, Ser247 (6.52) of the hA<sub>3</sub> receptor subtype is not present in the corresponding position of hA<sub>1</sub> and hA<sub>2</sub> receptors, where the residue is replaced by a histidine (His251 in hA<sub>1</sub>, His250 in hA<sub>2A</sub>, and His251 in hA<sub>2B</sub>). The histidine side chain is bulkier than serine and, possibly for this reason,

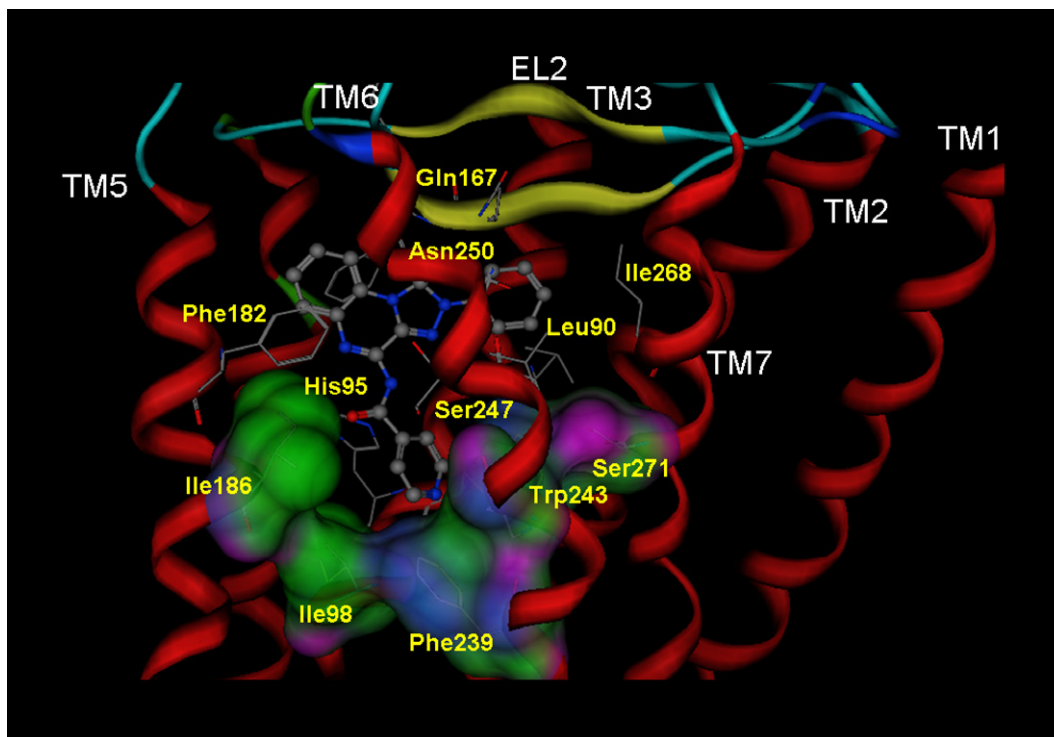


**Figure 4.** Hypothetical binding motif of the representative newly synthesized triazoloquinoxaline antagonists. The most energetically favorable docked conformation of derivative **4** into LBHM-model 1 is viewed from the membrane side facing TM helices 4 and 5. Side chains of some amino acids important for ligand recognition are highlighted. Hydrogen atoms are not displayed. Moreover, the receptor region around  $R_4$ -substituents characterized by five non-polar amino acids, Ile98 (TM3), Ile186 (TM5), Phe239 (TM6), Phe243 (TM5), and Ser271 (TM7), has been represented by its Connolly's molecular surface.

large substituents at the four-position of the triazoloquinoxaline framework are not well tolerated by  $hA_1$  and  $hA_2$  receptor subtypes. Indeed, 4-acylamino, 4-sulfonamido and 4-benzylureido derivatives are inactive or modestly active on  $hA_1$  and  $hA_{2A}$  ARs. On the contrary, the hydroxyl group of Ser247 (6.52) of the  $hA_3$  receptor is appropriately positioned to form a hydrogen-bonding interaction with the carbonyl oxygen of the 4-amido/sulfonamido/ureido group of compounds **A**, **1–19**. In particular, the 4-sulfonamido derivatives **13** and **14** interact simultaneously through hydrogen bonds with all three polar amino acids Thr94 (3.36), His95 (3.37), and Ser247 (6.52). Interestingly, also the 4-benzyloxy analogs **20–21** are selectively accommodated into the  $hA_3$  binding cavity. These observations support the importance of the group at the four-position in modulating receptor selectivity. Indeed, the receptor region around the  $R_4$ -substituent is mostly hydrophobic and characterized by five non-polar amino acids: Ile98 (3.40), Ile186 (5.47), Leu190 (5.51), Phe239 (6.44), and Leu244 (6.49), as shown in Figure 4.

Considering the observed structure–activity relationships in greater detail, methoxy substitution at  $R_1$  position is rather well tolerated among all newly synthesized triazoloquinoxaline derivatives. This is consistent with its accommodation into a tiny hydrophobic pocket delimited by Leu90 (3.32) and Ile268 (7.39). Interestingly, the amino acid corresponding to Leu90 in the  $hA_3$  receptor was found to be essential for the binding of both agonists and antagonists, and it is mutated in

valine (Val87) in the human  $A_1$  receptor. This mutation might explain the  $hA_3$  versus  $hA_1$  selectivity. In fact, even if the mutation Leu90 ( $hA_3$ )/Val87 ( $hA_1$ ) can slightly enlarge the dimension of this hydrophobic cavity, simultaneously it also sensibly decreases both shape and hydrophobic complementarities (data not shown). Also the mutation of Ser165 (EL2 of  $hA_3$ ) with Lys168 in the  $hA_1$  receptor could affect the recognition of the methoxy-substituted triazoloquinoxaline derivatives.

As previously described,<sup>22</sup> the presence of the 6-nitro substituent has not always produced advantageous effects in terms of  $hA_3$  AR binding affinity. This phenomenon is particularly evident comparing derivatives **6** and **12** with respect to their unsubstituted compounds **4** and **10**. As already anticipated and clearly shown in Figure 3, the relative position of  $R_6$ -substituent is slightly different depending on the bulkiness of the  $R_4$ -substituent on the carbamoyl moiety at the four-position. In particular, in the presence of a less bulky  $R_4$  substituent, the triazoloquinoxaline moiety binds more deeply in the middle of the TM bundle, positioning the 6-nitro substituent very close to TM5. In this case, unfavorable steric and dipolar interactions are responsible for the remarkable reduction of affinity observed for derivatives **6** and **12**. Increasing the bulkiness of the  $R_4$ -substituent, the position of the  $R_6$  group shifts away from TM5 and, consequently, more empty space is available for the 6-nitro substituent such as in derivatives **9** and **17**.

### 4.3. Electrophysiological studies

Compound **13** was also tested in an in vitro rat model of cerebral ischemia obtained by oxygen and glucose deprivation (OGD). During cerebral ischemia, extracellular adenosine concentration drastically increases both in vivo and in vitro<sup>36</sup> reaching a level able to stimulate all adenosine receptor subtypes, A<sub>1</sub>, A<sub>2A</sub>, A<sub>2B</sub>, and A<sub>3</sub>. Recently, it has been demonstrated that, in the CA1 hippocampus in vitro, the role played by A<sub>3</sub> receptors under ischemia depends upon the time duration of ischemic insults.<sup>37</sup> A<sub>3</sub> receptors stimulated by adenosine released during brief periods of ischemia, obtained by OGD, might exert A<sub>1</sub>-like protective effects on neurotransmission. On the contrary, prolonged periods of OGD would transform the A<sub>3</sub> receptor-mediated effects from protective to injurious.<sup>37</sup> The latter result is in agreement with that obtained in the same brain area<sup>13,23</sup> using different hA<sub>3</sub> AR and rA<sub>3</sub>AR antagonists.

An important factor in the study of brain ischemia is the generation of anoxic depolarization (AD), a consistent drop of neuron and glia membrane potential which may contribute to the amount and severity of neuronal damage<sup>38,39</sup> in this pathological condition. It has been suggested that a possible strategy in the development of neuroprotective drugs may include agents that inhibit the initiation or propagation of AD.

In the present study we investigated the effects of the newly synthesized compound **13** on synaptic transmission and AD development under OGD in the CA1 region of rat hippocampal slices. We examined the effects of 7 and 30 min OGD in the absence or presence of derivative **13**.

As shown in Figure 5A (left panel), 7-min OGD constantly elicited AD, recorded as negative d.c. (direct current) shifts, with a mean peak latency of  $6.3 \pm 0.3$  min from the beginning of ischemia and a peak amplitude of  $-7.7 \pm 0.8$  mV ( $n = 8$ ). In the presence of compound **13** (10 nM,  $n = 4$ ) AD was absent in all recorded slices (Fig. 5A, right panel). In addition, 7-min OGD elicited a complete loss of fEPSP amplitude which was prevented when OGD was carried out in the presence of compound **13** (Fig. 5B). The A<sub>3</sub> AR antagonist **13** was applied 15 min before, during, and 5 min after OGD. The compound did not change fEPSP amplitude under normoxic conditions (from  $1.0 \pm 0.04$  mV to  $0.97 \pm 0.05$  mV after 15 min application,  $n = 4$ ), but it induced a significant fEPSP recovery after OGD ( $100 \pm 2\%$ ,  $n = 4$ , in comparison to  $4.2 \pm 1.6\%$ ,  $n = 8$  found in untreated hippocampal slices). These findings are in agreement with our previous results showing that several, chemically diverse, A<sub>3</sub> receptor antagonists prevented the irreversible failure of neurotransmission induced by 7-min OGD and induced a complete AD abolishment or delay.<sup>13,25,37</sup>

It has to be noted that the most likely mechanism of fEPSP reduction in the CA1 hippocampus during ischemia is a decrease in glutamate release caused by activation of presynaptic A<sub>1</sub> receptors induced by extracellular

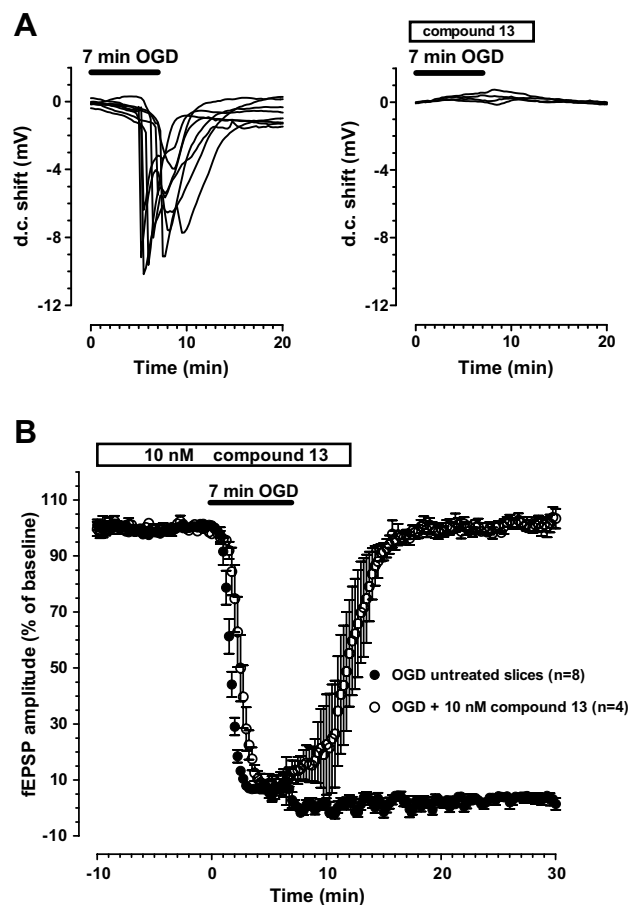


**Figure 5.** The selective A<sub>3</sub> antagonist **13** prevents the loss of neurotransmission induced by 7-min OGD. (A) AD was recorded as the negative d.c. shift in response to 7-min OGD (solid bar) in the absence ( $n = 8$ , left panel) and in the presence of 10 nM compound **13** (open bar,  $n = 4$ , right panel). Note that the A<sub>3</sub> antagonist completely prevented AD appearance. (B) Graphs show the time course of 7-min OGD (solid bar) effect on fEPSP amplitude, expressed as percentage of baseline, in untreated OGD slices (filled circles, means  $\pm$  SEM,  $n = 8$ ) or in the presence of 10 nM compound **13** (open circles, means  $\pm$  SEM,  $n = 4$ ). Solid bars indicate the duration of OGD.

adenosine. This effect is detectable by first 2 min of ischemia.<sup>40</sup> Nevertheless, at the concentration used in our experiments, the A<sub>1</sub> antagonistic effect of compound **13** ( $K_i = 132 \pm 12$  nM) did not appear since the compound did not modify the depression of fEPSP induced by OGD (Fig. 5B).

In order to well-define the effects of compound **13** on AD development, we prolonged the duration of ischemic insult from 7 to 30 min, a time duration able to induce an irreversible loss of neurotransmission in the CA1 hippocampus in vitro.<sup>13</sup> In untreated slices, 30-min OGD always elicited AD with a mean peak time of  $6.9 \pm 0.3$  min ( $n = 11$ ), measured from the beginning of ischemic insult, and an amplitude of  $-7.6 \pm 0.8$  mV (Fig. 6A). Compound **13** (10 nM,  $n = 11$ ), applied 15 min before and during OGD, induced a significant delay in AD appearance ( $9.3 \pm 0.5$  min,  $P = 0.0006$ , Fig. 6A and B), without producing any considerable change in AD amplitude ( $-6.3 \pm 0.7$  mV). Compound

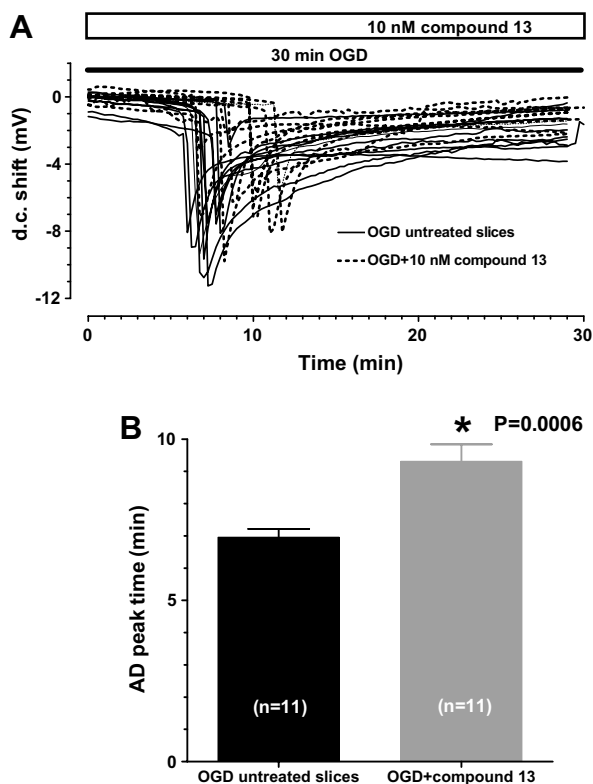


**Figure 6.** The selective  $A_3$  antagonist **13** delays the appearance of AD elicited by 30-min OGD in the CA1 region of rat hippocampal slices. (A) Traces are recordings of negative d.c. shifts in response to 30-min OGD taken from hippocampal slices in the absence ( $n = 11$ , continuous lines) or in the presence of **13** at 10 nM concentration (open bar,  $n = 11$ , dotted lines). Note that in the presence of the selective  $A_3$  adenosine receptor antagonist the appearance of AD was always delayed in comparison to that obtained in the absence of the drug. (B) Columns represent means  $\pm$  SEM of AD peak time recorded in hippocampal slices during 30-min OGD application, measured from the beginning of ischemic insult. Compound **13** significantly postponed AD development. \* $P = 0.0006$ , unpaired two-tailed Student's  $t$  test. ( $n$ ) indicates the number of tested slices.

**13** was ineffective on AD appearance at a concentration of 0.5 nM ( $n = 2$ , AD peak time of  $\sim 7$  min, data not shown), while a significant effect started from 1 nM ( $n = 3$  AD peak time of  $8.7 \pm 0.5$ , data not shown). No increase in the effect of compound **13** was observed up to the concentration of 1  $\mu$ M ( $n = 3$ , AD peak time of  $9.2 \pm 0.5$  min, data not shown). After 30-min OGD carried out in the presence of derivative **13**, no recovery of fEPSP amplitude was observed also after prolonged (40 min  $n = 3$ , data not shown) reperfusion in normal oxygenated aCSF (artificial cerebral spinal fluid).

During OGD conditions adenosine is released from hippocampal slices, reaching at the receptors concentrations up to 30  $\mu$ M after 5-min OGD.<sup>40,41</sup> These concentrations can stimulate  $A_3$  ARs which have affinity in the micromolar range for adenosine.<sup>42</sup> We demonstrated that compound **13** permits the recovery of synaptic activity after an otherwise irreversible ischemic insult (7-min duration) and delays the occurrence of AD brought about by a prolonged period of OGD. This re-

sult would appear to be in discrepancy with the very low  $rA_3$  AR binding affinity of **13**. However, it is consistent with previous findings showing that in the same in vitro model, other  $A_3$  antagonists,<sup>13,26,37</sup> such as (2*R*,3*R*,4*S*)-2-(2-chloro-6-(3-iodobenzylamino)-9*H*-purin-9-yl)tetrahydrothiophene-3,4-diol (LJ 1251),<sup>43</sup> 3-propyl 6-ethyl-5-[(ethylthio)carbonyl]-2-phenyl-4-propyl-3-pyridinecarboxylate (MRS 1523),<sup>44</sup> *N*-[9-chloro-2-(2-furanyl)-1,2,4-triazolo[1,5-*c*]quinazolin-5-yl]benzeneacetamide (MRS 1220)<sup>45</sup> and 5-[[4-(pyridyl)amino]carbonyl]amino-8-methyl-2-(2-furyl)-pyrazolo[4,3-*e*]-1,2,4-triazolo[1,5-*c*]pyrimidine hydrochloride,<sup>46</sup> and 4-amido-2-phenylpyrazolo[3,4-*c*]quinoline derivatives<sup>23</sup> led to recovery of synaptic activity after 7-min OGD at nanomolar concentration. Among them, only MRS 1523 and LJ 1251 possessed nanomolar affinity for the  $rA_3$  AR ( $K_i = 113$  and 3.89 nM, respectively).<sup>43,44</sup> As already discussed,<sup>37</sup> the apparent discrepancy between the  $rA_3$  binding affinity of compound **13** and its protective effect on OGD, observed at 10 nM concentration, might depend on the specific environment and coupling of  $A_3$  receptors in the cell membrane of native tissue and may differ from that assessed in receptor binding experiments. Alternatively, the paucity of  $A_3$  AR in native tissue,<sup>47,48</sup> allows one to speculate that occupancy of a substantial fraction of  $A_3$  receptors is required to evoke cell response(s). Thus, the blockage of a relatively small fraction of  $A_3$  receptors may be sufficient to antagonize the effect of endogenous adenosine released during OGD.

There is growing evidence that during ischemia the development of AD can be an important determinant of the degree and extent of ischemic damage and that NMDA receptors are essential to AD initiation and propagation.<sup>39</sup> The time-window of  $A_3$  receptor-mediated effects found in the present work, and also reported by Pugliese et al.,<sup>13,37</sup> overlaps with the delay that can be obtained by treating the slices with glutamate receptor antagonists.<sup>49,50</sup> On this basis, we suppose that the postponement of AD appearance caused by derivative **13** may be attributable to reduction in excitotoxic glutamate effect. Rat cortical neurons exposed to hypoxia in vitro show an increase in activation of protein kinase C (PKC) after selective  $A_3$  receptor stimulation.<sup>51</sup> It has been demonstrated that in the CA1 region of rat hippocampal slices the activation of  $A_3$  adenosine receptors reduces the inhibitory function of metabotropic glutamate receptors on glutamate excitotoxic effect.<sup>52</sup> Overall, these mechanisms may contribute to a deleterious role of prolonged stimulation of  $A_3$  receptors during ischemia.

## 5. Conclusion

The present study afforded new potent  $hA_3$  AR antagonists (compounds **7–8**, **13**, **16**, **17**, **20–21**), belonging to the class of the 2-aryl-1,2,4-triazolo[4,3-*a*]quinoxaline-1-ones, which also showed high selectivities versus both  $hA_1$  and  $hA_{2A}$  ARs.

Molecular docking studies, carried out using a ligand-based homology modeling approach, led to the identifi-

cation of the putative binding mode of the new derivatives which was coherent with the observed SAR. Compound **13**, tested in an in vitro rat model of cerebral ischemia, prevented the irreversible failure of the neurotransmission caused by a 7-min ischemic insult and delayed the occurrence of AD induced by a prolonged (30-min) period of OGD. These results show that derivative **13** might be efficacious in ameliorating the resistance of the CA1 region of hippocampus to ischemic damage.

## 6. Experimental

### 6.1. Chemistry

Silica gel plates (Merck  $F_{254}$ ) and silica gel 60 (Merck, 70–230 mesh) were used for analytical and column chromatography, respectively. All melting points were determined on a Gallenkamp melting point apparatus. Microanalyses were performed with a Perkin-Elmer 260 elemental analyzer for C, H, N, and the results (reported in Table 2) were within  $\pm 0.4\%$  of the theoretical values, unless otherwise stated. The IR spectra were recorded with a Perkin-Elmer Spectrum RX I spectrometer in Nujol mulls and are expressed in  $\text{cm}^{-1}$ . The  $^1\text{H}$  NMR spectra were obtained with a Bruker Avance 400 MHz instrument. The chemical shifts are reported in  $\delta$  (ppm) and are relative to the central peak of the solvent which was DMSO- $d_6$ . The following abbreviations are used: *s* = singlet, *d* = doublet, *dd* = double doublet, *t* = triplet, *m* = multiplet, *br* = broad, and *ar* = aromatic protons.

**6.1.1. General procedure for the synthesis of 2-aryl-4-(4-carbomethoxybenzoylamino)-1,2-dihydro-1,2,4-triazolo[4,3-*a*]quinoxalin-1-ones (1–2).** A solution of 4-carbomethoxybenzoyl chloride<sup>53</sup> (2.6 mmol) in anhydrous pyridine (2 mL) was added to a suspension of **22–23**<sup>16</sup>

(1.3 mmol) in anhydrous pyridine (6 mL). The mixture was refluxed for about 10–15 h. After cooling at room temperature, the mixture was diluted with water (30 mL) and the solid collected by filtration.

**Compound 1:** Yield: 83%; mp 251–252 °C (DMF).  $^1\text{H}$  NMR 3.93 (s, 3H, OMe), 7.38 (t, 1H, ar,  $J = 7.4$  Hz), 7.54–7.68 (m, 4H, ar), 7.79 (d, 1H, ar), 8.02 (d, 2H, ar,  $J = 8.4$  Hz), 8.13–8.20 (m, 4H, ar), 8.79 (d, 1H, H-9,  $J = 8.1$  Hz), 11.48 (br s, 1H, NH). IR 1727.

**Compound 2:** Yield: 90%; mp 256–258 °C (DMF).  $^1\text{H}$  NMR 3.09 (s, 3H, OMe), 3.79 (s, 3H, COOMe), 7.09 (d, 2H, ar,  $J = 7.0$  Hz), 7.52–7.89 (m, 5H, ar), 8.08–8.18 (m, 4H, ar), 8.75 (d, 1H, H-9,  $J = 8.1$  Hz), 11.51 (br s, 1H, NH). IR 1713.

**6.1.2. 4-(3-Iodobenzoylamino)-1,2-dihydro-2-phenyl-1,2,4-triazolo[4,3-*a*]quinoxalin-1-one (3).** A solution of 3-iodobenzoyl chloride<sup>54</sup> (3.38 mmol) in anhydrous dichloromethane (5 mL) was added to a suspension of **22**<sup>16</sup> (0.68 mmol) in anhydrous dichloromethane (20 mL) and anhydrous pyridine (9.8 mmol, 0.7 mL). The mixture was refluxed for 3 h. Evaporation of the solvent at reduced pressure gave a residue which was treated with water/ethanol, collected by filtration and washed with water. Yield: 79%; mp 286–287 °C (AcOH/DMF).  $^1\text{H}$  NMR 7.38–7.98 (m, 6 H, ar), 7.79 (d, 1H,  $J = 8.1$  Hz), 7.98–8.02 (m, 4H, ar), 8.37 (s, 1H, ar), 8.76 (d, 1H, H-9,  $J = 8.1$  Hz), 11.35 (br s, 1H, NH). IR 1680, 1735, 3225.

**6.1.3. General procedure for the synthesis of 2-aryl-4-(4-pyridylcarbonylamino)-1,2-dihydro-1,2,4-triazolo[4,3-*a*]quinoxalin-1-ones (4–6).** A solution of 4-pyridylcarbonylchloride<sup>55</sup> (2.6 mmol) in anhydrous pyridine (2 mL) was added dropwise at room temperature to a suspension of compounds **22–24**<sup>16,17</sup> (1.3 mmol) in anhydrous pyridine (10 mL). The mixture was refluxed for about

**Table 2.** Combustion Analysis data of the newly synthesized compounds

Compound	Formula	C		H		N	
		Calcd	found	Calcd	found	Calcd	found
<b>1</b>	C <sub>24</sub> H <sub>17</sub> N <sub>5</sub> O <sub>4</sub>	65.60	65.74	3.90	3.78	15.94	16.10
<b>2</b>	C <sub>25</sub> H <sub>19</sub> N <sub>5</sub> O <sub>5</sub>	63.96	63.79	4.08	4.23	14.92	14.75
<b>3</b>	C <sub>22</sub> H <sub>14</sub> I N <sub>5</sub> O <sub>2</sub>	52.09	51.05	2.78	2.59	13.81	14.01
<b>4</b>	C <sub>21</sub> H <sub>14</sub> N <sub>6</sub> O <sub>2</sub>	65.96	66.15	3.69	3.88	21.98	22.10
<b>5</b>	C <sub>22</sub> H <sub>16</sub> N <sub>6</sub> O <sub>3</sub>	64.07	64.28	3.91	3.75	20.38	20.10
<b>6</b>	C <sub>21</sub> H <sub>13</sub> N <sub>7</sub> O <sub>4</sub>	59.02	58.94	3.07	3.20	22.94	22.78
<b>7</b>	C <sub>21</sub> H <sub>15</sub> N <sub>5</sub> O <sub>3</sub> S	60.42	60.20	3.62	3.82	16.78	16.99
<b>8</b>	C <sub>22</sub> H <sub>17</sub> N <sub>5</sub> O <sub>4</sub> S	59.05	58.94	3.83	3.60	15.65	15.44
<b>9</b>	C <sub>21</sub> H <sub>14</sub> N <sub>6</sub> O <sub>5</sub> S	54.54	54.78	3.05	3.19	18.17	18.24
<b>10</b>	C <sub>16</sub> H <sub>13</sub> N <sub>5</sub> O <sub>3</sub> S	54.08	54.20	3.69	3.88	19.71	19.54
<b>11</b>	C <sub>17</sub> H <sub>15</sub> N <sub>5</sub> O <sub>4</sub> S	52.98	53.12	3.92	3.74	18.17	18.01
<b>12</b>	C <sub>16</sub> H <sub>12</sub> N <sub>6</sub> O <sub>5</sub> S	48.00	48.23	3.02	3.25	20.99	20.78
<b>13</b>	C <sub>17</sub> H <sub>15</sub> N <sub>5</sub> O <sub>5</sub> S <sub>2</sub>	47.10	47.32	3.49	3.60	16.16	16.25
<b>14</b>	C <sub>18</sub> H <sub>17</sub> N <sub>5</sub> O <sub>6</sub> S <sub>2</sub>	46.64	46.39	3.70	3.91	15.11	14.91
<b>15</b>	C <sub>23</sub> H <sub>18</sub> N <sub>6</sub> O <sub>2</sub>	67.31	67.23	4.42	4.65	20.48	20.30
<b>16</b>	C <sub>24</sub> H <sub>20</sub> N <sub>6</sub> O <sub>3</sub>	65.45	65.27	4.58	4.81	19.08	19.29
<b>17</b>	C <sub>23</sub> H <sub>17</sub> N <sub>7</sub> O <sub>4</sub>	60.66	60.40	3.76	3.90	21.53	21.42
<b>19</b>	C <sub>22</sub> H <sub>15</sub> IN <sub>6</sub> O <sub>2</sub>	50.59	50.38	2.89	2.70	16.09	16.31
<b>20</b>	C <sub>22</sub> H <sub>16</sub> N <sub>4</sub> O <sub>2</sub>	71.73	71.58	4.38	4.61	15.21	15.39
<b>21</b>	C <sub>23</sub> H <sub>18</sub> N <sub>4</sub> O <sub>3</sub>	69.34	69.66	4.55	4.70	14.06	14.29

20 h. After cooling at room temperature the solution was diluted with water (30 mL) and the solid precipitate was filtered.

**Compound 4:** Yield: 85%; mp 273–275 °C (DMF).  $^1\text{H}$  NMR 7.25–7.37 (m, 1H, ar), 7.42–7.82 (m, 5H, ar), 7.85–8.02 (m, 4H, 2-pyridine protons + 2 ar), 8.73–8.82 (m, 3H, 2 pyridine protons + H-9), 11.82 (br s, 1H, NH). IR 1670, 1728, 3214.

**Compound 5:** Yield: 80%; mp 220–222 °C (DMF).  $^1\text{H}$  NMR 3.78 (s, 3H, OMe), 7.09 (d, 2H, ar,  $J = 9.2$  Hz), 7.25–7.92 (m, 7H, ar), 8.72–8.82 (m, 3H, 2 pyridine protons + H-9), 11.65 (br s, 1H, NH). IR 1723.

**Compound 6:** Yield: 97%; mp >300 °C (DMF).  $^1\text{H}$  NMR 7.37–7.63 (m, 3H, ar), 7.72–8.06 (m, 6H, ar), 8.78–8.98 (m, 3H, 2 pyridine protons + H-9), 11.77 (s, 1H, NH). IR 1715.

**6.1.4. General procedure for the synthesis of 4-benzenesulfonylamino-1,2-dihydro-2-phenyl-1,2,4-triazolo[4,3-*a*]quinoxalin-1-one (7) and 4-benzenesulfonylamino-1,2-dihydro-2-(4-methoxyphenyl)-1,2,4-triazolo[4,3-*a*]quinoxalin-1-one (8).** A mixture of compound **22** or **23**<sup>16</sup> (1.08 mmol) and benzenesulfonylchloride (14 mmol, 1.78 mL) in anhydrous dichloromethane (30 mL) and anhydrous pyridine (15 mmol, 1.2 mL) was refluxed until the disappearance of the starting 4-amino derivative (3–6 days). The mixture was cooled at room temperature and the solid collected by filtration and washed with water.

**Compound 7:** Yield: 64%; mp >300 °C (DMF).  $^1\text{H}$  NMR 7.36–7.66 (m, 9H, ar), 7.97 (d, 2H, ar,  $J = 6.2$  Hz), 8.01–8.05 (m, 2H, ar), 8.62–8.66 (m, 1H, H-9), 11.4 (br s, 1H, NH). IR 1720, 3300.

**Compound 8:** Yield: 77%; mp >300 °C (DMF).  $^1\text{H}$  NMR 3.78 (s, 3H, OMe), 7.07 (d, 2H, ar,  $J = 9.2$  Hz), 7.37–7.42 (m, 2H, ar), 7.44–8.06 (m, 8H, ar), 8.59–8.65 (m, 1H, H-9), 11.5 (br s, 1H, NH). IR 1723, 3266.

**6.1.5. 4-Benzenesulfonylamino-1,2-dihydro-6-nitro-2-phenyl-1,2,4-triazolo[4,3-*a*]quinoxalin-1-one (9).** A mixture of compound **24**<sup>17</sup> (0.9 mmol) and benzenesulfonylchloride (2.6 mmol, 0.20 mL) in anhydrous pyridine (5 mL) was refluxed for 36 h. After cooling at room temperature, the solid was collected by filtration and washed with water. Yield: 81%; mp 222–224 °C (DMF).  $^1\text{H}$  NMR 7.37–7.64 (m, 7H, ar), 7.96–8.21 (m, 5H, ar), 8.99 (d, 1H, H-9,  $J = 7.8$  Hz), 11.3 (br s, 1H, NH). IR 1378, 1536, 1717, 3125.

**6.1.6. 1,2-Dihydro-4-methanesulfonylamino-2-phenyl-1,2,4-triazolo[4,3-*a*]quinoxalin-1-one (10).** A solution of methanesulfonyl chloride (2.52 mmol, 0.2 mL) in anhydrous pyridine (1 mL) was added at room temperature to a suspension of compound **22**<sup>16</sup> (2.52 mmol, 0.7 g) in anhydrous pyridine (10 mL). The mixture was refluxed for 12 h, then a second portion of methanesulfonyl chloride (5 mmol, 0.4 mL) in anhydrous pyridine (1 mL) was added and the reflux continued. Further five

additions of the same quantity of methanesulfonyl chloride (5 mmol, 0.4 mL) were done every 12 h, for a total reflux time of about 90 h. After cooling, the mixture was taken up with water (20 mL) and the resulting solid was collected by filtration and washed with water. The crude solid was purified by column chromatography, (SiO<sub>2</sub>, eluting system cyclohexane/ethyl acetate/methanol, 4.5:4.5:0.5). Evaporation of the second eluates gave a solid which was recrystallized from 2-methoxyethanol. Yield: 30%; mp 270–272 °C.  $^1\text{H}$  NMR 3.33 (s, 3H, SO<sub>2</sub>CH<sub>3</sub>), 7.37–7.43 (m, 3H, ar), 7.56–7.60 (m, 2H, ar), 7.87–8.03 (m, 3H, ar), 8.63–8.67 (m, 1H, H-9), 11.50 (br s, 1H, NH). IR 1644, 1734, 3181.

**6.1.7. 1,2-Dihydro-4-methanesulfonylamino-2-(4-methoxyphenyl)-1,2,4-triazolo[4,3-*a*]quinoxalin-1-one (11).** A solution of methanesulfonyl chloride (6.5 mmol, 0.5 mL) in anhydrous dichloromethane (5 mL) was added at room temperature to a suspension of compound **23**<sup>16</sup> (0.65 mmol, 0.2 g) in anhydrous dichloromethane (30 mL) and anhydrous pyridine (9.1 mmol, 0.71 mL). The mixture was refluxed for 6 h and then a second portion of methanesulfonyl chloride (9.1 mmol, 0.72 mL) in anhydrous dichloromethane (5 mL) was added. The suspension was heated at reflux for further 8 h. After cooling at room temperature, the solid was collected by filtration and washed with water and washed with water. Yield: 50%; mp 278–280 °C (acetonitrile).  $^1\text{H}$  NMR 3.33 (s, 3H, SO<sub>2</sub>Me), 3.80 (s, 3H, OMe), 7.11 (d, 2H, ar,  $J = 8.8$  Hz), 7.38–7.43 (m, 2H, ar), 7.78–7.89 (m, 3H, ar), 8.62–8.67 (m, 1H, H-9), 11.45 (br s, 1H, NH). IR 1157, 1278, 1723, 3190.

**6.1.8. 1,2-Dihydro-4-methanesulfonylamino-6-nitro-2-phenyl-1,2,4-triazolo[4,3-*a*]quinoxalin-1-one (12).** A mixture of compound **24**<sup>17</sup> (0.77 mmol) and methanesulfonyl chloride (58.4 mmol, 4.5 mL) in anhydrous dichloromethane (30 mL) and anhydrous pyridine (10.5 mmol, 0.83 mL) was refluxed for 24 h. Then, a second portion of methanesulfonyl chloride (58.4 mmol, 4.5 mL) was added to the mixture and, after refluxing for 24 h, a third portion of the same amount of methanesulfonyl chloride was added. The suspension was heated for further 24 h and then cooled at room temperature. The solid was collected by filtration and washed with water. Yield: 40%; mp >300 °C (AcOH).  $^1\text{H}$  NMR 3.27 (s, 3H, SO<sub>2</sub>Me), 7.38 (t, 1H, ar,  $J = 7.3$  Hz), 7.58–7.66 (m, 3H, ar), 8.02 (d, 2H, ar,  $J = 8.1$  Hz) 8.10–8.18 (m, 1H, ar), 9.01 (d, 1H, H-9,  $J = 7.7$  Hz). IR 1121, 1295, 1376, 1533, 1722, 3110.

**6.1.9. 1,2-Dihydro-4-bismethanesulfonylamino-2-phenyl-1,2,4-triazolo[4,3-*a*]quinoxalin-1-one (13).** A mixture of compound **22**<sup>16</sup> (0.75 mmol) and methanesulfonyl chloride (15.4 mmol, 1.19 mL) in anhydrous dichloromethane (30 mL) and anhydrous pyridine (10.5 mmol, 0.83 mL) was refluxed for 15 h. After evaporation of the solvent at reduced pressure, the residue was taken up with water (10 mL) and the solid collected by filtration. Yield: 85%; mp 277–278 °C (DMF/EtOH).  $^1\text{H}$  NMR 3.88 (s, 6H, 2SO<sub>2</sub>Me), 7.41 (t, 1H, ar,  $J = 7.3$  Hz), 7.55–7.71 (m, 3H, ar), 7.86 (t, 1H, ar,  $J = 7.3$  Hz), 8.02–8.08 (m, 3H, ar), 8.79 (d, 1H, H-9,  $J = 8.1$  Hz). IR 1730.

**6.1.10. 1,2-Dihydro-4-bismethanesulfonylamino-2-(4-methoxyphenyl)-1,2,4-triazolo[4,3-*a*]quinoxalin-1-one (14).** The title compound was prepared by heating compound **23**<sup>16</sup> (0.65 mmol) and methanesulfonyl chloride (42 mmol, 3.2 mL) in anhydrous dichloromethane (30 mL) and anhydrous pyridine (10.5 mmol, 0.83 mL) at reflux for 38 h. Evaporation of the solvent at reduced pressure afforded a residue which was treated with water (10 mL). The solid was collected by filtration. Yield: 60%; mp 285–287 °C (EtOAc). <sup>1</sup>H NMR 3.81 (s, 3H, OMe), 3.86 (s, 6H, 2SO<sub>2</sub>Me), 7.12 (d, 2H, ar, *J* = 9.1 Hz), 7.61–7.94 (m, 4 H, ar), 8.04 (d, 1H, ar, *J* = 8.1 Hz), 8.78 (d, 1H, H-9, *J* = 8.4 Hz). IR 1717.

**6.1.11. General procedure for the synthesis of 4-benzylureido-1,2-dihydro-2-phenyl-1,2,4-triazolo[4,3-*a*]quinoxalin-1-one (15), 4-benzylureido-1,2-dihydro-2-(4-methoxyphenyl)-1,2,4-triazolo[4,3-*a*]quinoxalin-1-one (16), and 4-benzylureido-1,2-dihydro-6-nitro-2-phenyl-1,2,4-triazolo[4,3-*a*]quinoxalin-1-one (17).** Benzylisocyanate (3.25 mmol) was added to a hot solution of the 4-amino derivative **22**, **23**<sup>16</sup> or **24**<sup>17</sup> (1.3 mmol) in anhydrous tetrahydrofuran (10 mL), under nitrogen atmosphere. The mixture was refluxed for about 3–5 h. After cooling at room temperature, the solid was collected by filtration and washed with water and diethyl ether.

Compound **15**: Yield: 55%; mp 258–260 °C (DMF). <sup>1</sup>H NMR 4.60 (d, 2H, CH<sub>2</sub>, *J* = 4.8 Hz), 7.22–7.73 (m, 11H, ar), 8.18 (d, 2H, ar, *J* = 8.7 Hz), 8.61 (d, 1H, H-9, *J* = 8.2 Hz), 9.72 (br s, 1H, NH), 9.87 (br s, 1H, NH).

Compound **16**: Yield: 62%; mp 245–247 °C (DMF). <sup>1</sup>H NMR 3.79 (s, 3H, OMe), 4.53 (d, 2H, CH<sub>2</sub>, *J* = 4.8 Hz), 7.09 (d, 2H, ar, *J* = 8.8 Hz), 7.20–7.45 (m, 7H, ar), 7.65–7.66 (m, 1H, ar), 8.02 (d, 2H, ar, *J* = 8.8 Hz), 8.63 (d, 1H, H-9, *J* = 8.1 Hz), 9.77 (br s, 1H, NH), 9.86 (br s, 1H, NH). IR 1682, 1718, 3192.

Compound **17**: Yield: 85%; mp 256–258 °C (DMF). <sup>1</sup>H NMR 4.50 (d, 2H, CH<sub>2</sub>, *J* = 5.1 Hz), 7.22–7.65 (m, 9H, ar), 8.02 (d, 1H, ar, *J* = 8.1 Hz), 8.15 (d, 2H, ar, *J* = 8.0 Hz), 8.89 (d, 1H, H-9, *J* = 8.2 Hz), 9.82 (br s, 1H, NH), 10.66 (br s, 1H, NH). IR 1686, 1729, 3184.

**6.1.12. 4-Benzoylureido-1,2-dihydro-2-phenyl-1,2,4-triazolo[4,3-*a*]quinoxalin-1-one (18).** A mixture of derivative **22**<sup>16</sup> (1.5 mmol) and benzoylisocyanate (2.32 mmol) in anhydrous tetrahydrofuran was refluxed for 6 h under nitrogen atmosphere. The suspension was cooled at room temperature, the solid was collected by filtration, and washed with diethyl ether. It was not possible to purify the crude compound **18** since it resulted unstable upon heating. In fact, recrystallization from nitromethane or DMF caused, respectively, its partial and total degradation to the starting 4-amino derivative. Nevertheless, TLC analysis (CHCl<sub>3</sub>/MeOH 9.5:0.5), <sup>1</sup>H NMR spectrum, and melting point of crude **18** showed that it was pure enough to be tested in the binding assays. Yield: 82%; mp 242–243 °C (crude). <sup>1</sup>H NMR 7.39–7.78 (m, 9H, ar), 8.06–8.09 (m, 4H, ar), 8.75 (d,

1H, H-9, *J* = 8.1 Hz), 11.5 (br s, 1H, NH), 12.5 (br s, 1H, NH). IR 1695, 1730, 3300.

**6.1.13. 1,2-Dihydro-4-(3-iodophenylureido)-2-phenyl-1,2,4-triazolo[4,3-*a*]quinoxalin-1-one (19).** 3-Iodophenylisocyanate (1.3 mmol) was added to a hot solution of derivative **22**<sup>16</sup> (0.9 mmol) in anhydrous tetrahydrofuran (10 mL), under nitrogen atmosphere. The mixture was refluxed for 3 h. After cooling at room temperature, the solid was collected by filtration and washed with water and diethyl ether. Yield: 95%; mp 225–226 °C (AcOH). <sup>1</sup>H NMR 7.18–7.65 (m, 8H, ar), 7.82–7.98 (m, 1H, ar), 8.15–8.30 (m, 3H, ar), 8.50–8.65 (m, 1H, H-9), 11.05 (br s, 1H, NH), 12.01 (br s, 1H, NH). IR 1690, 1730, 3180, 3290.

**6.1.14. General Procedure for the synthesis of 4-benzyl-oxy-1,2-dihydro-2-aryl-1,2,4-triazolo[4,3-*a*]quinoxalin-1-ones (20–21).** A suspension of sodium hydride (60% dispersion in mineral oil, 2.28 mmol) in anhydrous dimethylsulfoxide (7 mL) was stirred at 60 °C for 1 h, under nitrogen atmosphere. After cooling the suspension at 40 °C, benzyl alcohol (2.28 mmol, 0.23 mL) was added. The temperature of the mixture was left to rise to 20 °C, then a solution of the 4-chloro derivative **25**<sup>16</sup> or **26**<sup>16</sup> (1.9 mmol) in anhydrous dimethylsulfoxide (3 mL) was slowly added, keeping the temperature of the reaction at 20 °C. After the addition was completed, the mixture was stirred for about 12–15 h at room temperature, then it was diluted with water (20 mL). The solution was extracted with chloroform (3 × 30 mL). The organic phases were collected, washed with water (3 × 30 mL), and anhydri-fied (Na<sub>2</sub>SO<sub>4</sub>). Evaporation of the solvent at reduced pressure gave an oil residue which when treated with diethyl ether solidified. The solid was collected by filtration and purified by column chromatography (SiO<sub>2</sub>, eluting system CHCl<sub>3</sub>/EtOAc, 10:1).

Compound **20**: Yield: 35%; mp 168–169 °C (nitromethane). <sup>1</sup>H NMR 5.64 (s, 2H, CH<sub>2</sub>), 7.35–7.64 (m, 11H, ar), 8.01 (d, 2H, ar, *J* = 7.7 Hz), 8.71 (dd, 1H, H-9, *J* = 8.4, 2.6 Hz). IR 1730.

Compound **21**: Yield: 48%; mp 200–202 °C (AcOH). <sup>1</sup>H NMR 3.89 (s, 3H, OMe), 5.61 (s, 2H, CH<sub>2</sub>), 7.07 (d, 2H, ar, *J* = 7.3 Hz), 7.35–7.88 (m, 10H, ar), 8.67 (d, 1H, H-9, *J* = 8.2 Hz). IR 1716.

## 6.2. Computational methodologies

All modeling studies were carried out on a 10 CPU (PIV-3.0 GHz and AMD64) linux cluster running under openMosix architecture.<sup>56</sup>

Homology modeling, energy calculation, and docking studies were performed using the Molecular Operating Environment (MOE, version 2006.08) suite.<sup>57</sup>

All docked structures were fully optimized without geometry constraints using RHF/AM1 semi-empirical calculations. Vibrational frequency analysis was used to characterize the minima stationary points (zero imaginary frequencies). The software package MOPAC

(ver.7),<sup>58</sup> implemented in MOE suite, was utilized for all quantum mechanical calculations.

**6.2.1. Homology model of the human A<sub>3</sub> AR.** Based on the assumption that GPCRs share similar TM boundaries and overall topology, a homology model of the hA<sub>3</sub> receptor was constructed. First, the amino acid sequences of TM helices of the A<sub>3</sub> receptor were aligned with those of bovine rhodopsin, guided by the highly conserved amino acid residues, including the DRY motif (D3.49, R3.50, and Y3.51) and three proline residues (P4.60, P6.50, and P7.50) in the TM segments of GPCRs. The same boundaries were applied for the TM helices of the A<sub>3</sub> receptor as they were identified from the X-ray crystal structure for the corresponding sequences of bovine rhodopsin,<sup>59</sup> the C<sub>R</sub> coordinates of which were used to construct the seven TM helices for the hA<sub>3</sub> receptor. The loop domains of the hA<sub>3</sub> receptor were constructed by the loop search method implemented in MOE. In particular, loops are modeled first in random order. For each loop, a contact energy function analyzes the list of candidates collected in the segment searching stage, taking into account all atoms already modeled and any atoms specified by the user as belonging to the model environment. These energies are then used to make a Boltzmann-weighted choice from the candidates, the coordinates of which are then copied to the model. Any missing side-chain atoms are modeled using the same procedure. Side chains belonging to residues the coordinates of which were copied from a template are modeled first, followed by side chains of modeled loops. Outgaps and their side chains are modeled last. Special caution has to be given to the second extracellular (EL2) loop, which has been described in bovine rhodopsin as folding back over transmembrane helices<sup>59</sup> and, therefore, limiting the size of the active site. Hence, amino acids of this loop could be involved in direct interactions with the ligands. A driving force to this peculiar fold of the EL2 loop might be the presence of a disulfide bridge between cysteines in TM3 and EL2. Since this covalent link is conserved in all receptors modeled in the current study, the EL2 loop was modeled using a rhodopsin-like constrained geometry around the EL2-TM3 disulfide bridge. After the heavy atoms were modeled, all hydrogen atoms were added, and the protein coordinates were then minimized with MOE using the AMBER94 force field.<sup>60</sup> The minimizations were carried out by the 1000 steps of steepest descent followed by conjugate gradient minimization until the rms gradient of the potential energy was less than 0.1 kcal mol<sup>-1</sup> Å<sup>-1</sup>. Protein stereochemistry evaluation was performed by several tools (Ramachandran and Chi plots measure phi/psi and chi1/chi2 angles, clash contact reports) implemented in MOE suite.<sup>57</sup>

**6.2.2. Ligand-based homology modeling.** We have recently revisited the rhodopsin-based model of the human A<sub>3</sub> receptor in its resting state (antagonist-like state), taking into account a novel strategy to simulate the possible receptor reorganization induced by the antagonist-binding.<sup>31</sup> We called this new strategy ligand-based homology modeling. Briefly, ligand-based homology modeling technique is an evolution of a con-

ventional homology modeling strategy that combined the Boltzmann-weighted randomized modeling procedure adapted from Levitt<sup>61</sup> with a specialized algorithm for the proper handling of insertions and deletions of any selected extra-atoms during the energy tests and minimization stages of the modeling procedure. The ligand-based option is very useful when one wishes to build a homology model in the presence of a ligand docked to the primary template, or other proteins known to be complexed with the sequence to be modeled. In this specific case, both model building and refinement take into account the presence of the ligand in terms of specific steric and chemical features. In order to generate an initial ensemble of ligand poses, a conventional docking procedure (see next section for details) with reduced van der Waals radii (equal to 75%) and an increased Coulomb-vdW cutoff (cutoff on 10 Å; cutoff on 12 Å) was performed. For each pose, a homology model is then generated to accommodate the ligand by reorienting nearby side chains. These residues and the ligand are then locally minimized. Finally, each ligand is re-docked into its corresponding low-energy protein structures and the resulting complexes are ranked according to MOEScore.<sup>57</sup>

Different quantitative measurements of molecular volume of the receptor binding cavities have been carried out using MOE suite.<sup>57</sup> Prediction of antagonist–receptor complex stability (in terms of corresponding pK<sub>i</sub> value) and the quantitative analysis for non-bonded intermolecular interactions (H-bonds, transition metal, water bridges, and hydrophobic) were calculated and visualized using several tools implemented into MOE suite.<sup>57</sup>

**6.2.3. Molecular docking of the hA<sub>3</sub> AR antagonists.** All antagonist structures were docked into the hypothetical TM binding site using the MOE-dock tool, part of the MOE suite. Searching is conducted within a user-specified 3D docking box (the standard protocol selects all atoms inside 12 Å from the center of mass of the binding cavity), using the Tabu Search<sup>62</sup> protocol (standard parameters are 1000 steps/run, 10 attempts/step, and 10 Tabu list length), and the MMFF94 force field<sup>63</sup> MOE-Dock performs a user-specified number of independent docking runs (50 in our specific case) and writes the resulting conformations and their energies in a molecular database file. The resulting docked complexes were subjected to MMFF94 energy minimization until the rms of conjugate gradient was <0.1 kcal mol<sup>-1</sup> Å<sup>-1</sup>. Charges for the ligands were imported from the MOPAC output files. To better refine all antagonist–receptor complexes, a rotamer exploration of all side chains involved in the antagonist-binding was carried out. Rotamer exploration methodology was implemented in MOE suite.<sup>57</sup>

## 6.3. Pharmacology

**6.3.1. Bovine A<sub>1</sub> and A<sub>2A</sub> receptor binding.** Displacement of [<sup>3</sup>H]DPCPX from A<sub>1</sub> ARs in bovine cortical membranes and [<sup>3</sup>H]CGS 21680 from A<sub>2A</sub> ARs in bovine striatal membranes was performed as described in Ref. 64 and Ref. 65, respectively.

**6.3.2. Human A<sub>1</sub>, A<sub>2A</sub>, and A<sub>3</sub> receptor binding.** Binding experiments at hA<sub>1</sub> and hA<sub>2A</sub> ARs, stably expressed in CHO cells, were performed as previously described in Ref. 66 using [<sup>3</sup>H]DPCPX and [<sup>3</sup>H]NECA, respectively, as radioligands. Displacement of [<sup>125</sup>I]AB-MECA from hA<sub>3</sub> AR, stably expressed in CHO cells, was performed as reported in Ref. 18.

**6.3.3. Rat A<sub>1</sub> receptor binding.** Rat brain cortex was dissected from male Wistar rats. Membrane preparation was carried out as previously reported for the bovine membrane preparation.<sup>65</sup> The A<sub>1</sub> binding assays were performed in triplicate by incubating aliquots of brain cortex membranes (40–50 μg of protein) at 25 °C for 180 min in 0.5 mL of binding buffer (50 mM Tris/HCl, 2 mM MgCl<sub>2</sub>, pH 7.7) containing 0.2–0.5 nM [<sup>3</sup>H]DPCPX. Non-specific binding was defined in the presence of 20 μM R-PIA. Incubation was terminated by rapid filtration through Whatman GF/C glass microfiber filters and washing twice with 4 mL of ice-cold buffer. K<sub>D</sub> value on brain cortex was 0.51 nM.<sup>67</sup>

**6.3.4. Rat A<sub>3</sub> receptor binding.** Binding of [<sup>3</sup>H] (R)-PIA (37 Ci/mmol) to rat testis membranes was measured in the presence of DPCPX (150 nM) as previously described.<sup>23,68</sup> Briefly, fresh testicular tissue from Wistar rats was dissected free of epididymis and membranes were prepared as described.<sup>68</sup> Rat testis membranes (0.1–0.2 mg of protein) and [<sup>3</sup>H] (R)-PIA 4 nM were incubated in 0.5 mL total volume of 50 mM Tris/HCl (pH 7.4), 1 mM EDTA, and 10 mM MgCl<sub>2</sub> buffer in the presence of 150 nM DPCPX to block A<sub>1</sub> adenosine receptors. Non-specific binding was determined in the presence of 15 μM (R)-PIA. Binding reactions were terminated by filtration through Whatman GF/C filters under reduced pressure. Filters were washed three times with 5 mL of ice-cold buffer and introduced into scintillation vials. The radioactivity was counted in 4 mL of scintillation cocktail in a scintillation counter.

**6.3.5. Measurement of cAMP Levels on CHO cells transfected with human A<sub>2B</sub> and A<sub>3</sub> ARs.** Intracellular cAMP levels were measured using a competitive protein binding method.<sup>69</sup> CHO cells (~60,000), stably expressing hA<sub>2B</sub> or hA<sub>3</sub> ARs, were plated in 24-well plates. After 48 h, the medium was removed, and the cells were incubated at 37 °C for 15 min with 0.5 mL di DMEM in the presence of Ro 20-1724 (4-(3-butoxy-4-methoxybenzyl)imidazolidin-2-one) (20 μM) and adenosine deaminase (1U/mL). A stock 1 mM solution of the tested compound was prepared in DMSO, and subsequent dilutions were accomplished in distilled water. The antagonistic profile of the new compound toward hA<sub>2B</sub> AR was evaluated assessing its ability to inhibit 100 nM NECA-mediated accumulation of cAMP. The antagonistic profile of the new compound toward hA<sub>3</sub> AR was evaluated by assessing its ability to counteract 100 nM NECA-mediated inhibition of cAMP accumulation stimulated by 1 μM forskolin. Cells were incubated in the reaction medium (15 min at 37 °C) with different compound concentrations (1 nM–10 μM) and then treated with NECA. The reaction was terminated by remov-

ing the medium and adding 0.4 N HCl. After 30 min the lysate was neutralized with KOH 4 N and the suspension was centrifuged at 800g for 5 min. To determine cyclic AMP production, the binding protein, prepared from beef adrenal glands, was incubated with [<sup>3</sup>H]cAMP (2 nM) in distilled water, 50 μL of cell lysate, or standard cAMP (0–16 pmol) at 4 °C for 150 min in a total volume of 300 μL. Bound radioactivity was separated by rapid filtration through GF/C glass fiber filters and washed twice with 4 mL of 50 mM Tris/HCl, pH 7.4. The radioactivity was measured by liquid scintillation spectrometry.

**6.3.6. Data analysis.** The concentration of the tested compounds that produced 50% inhibition of specific [<sup>3</sup>H]DPCPX, [<sup>3</sup>H]NECA, [<sup>3</sup>H]CGS 21680 and [<sup>125</sup>I]AB-MECA binding (IC<sub>50</sub>) was calculated using a non-linear regression method implemented by the InPlot program (Graph-Pad, San Diego, CA, USA) with five concentrations of displacer, each performed in triplicate. Inhibition constants (K<sub>i</sub>) were calculated according to the Cheng–Prusoff equation.<sup>70</sup> The dissociation constant (K<sub>d</sub>) values of [<sup>3</sup>H] DPCPX and [<sup>3</sup>H]CGS 21680 in cortical and striatal bovine brain membranes were 0.3 nM and 14 nM, respectively. The K<sub>d</sub> values of [<sup>3</sup>H]DPCPX, [<sup>3</sup>H]NECA and [<sup>125</sup>I]AB-MECA in hA<sub>1</sub>, hA<sub>2A</sub> and hA<sub>3</sub> ARs in CHO cell membranes were 3 nM, 30 nM, and 1.4 nM, respectively. EC<sub>50</sub> values obtained in cAMP assays were calculated by non-linear regression analysis using the equation for a sigmoid concentration–response curve (Graph-Pad, San Diego, CA, USA).

**6.3.7. Electrophysiological assays: slice preparation.** All animal procedures were carried out according to the European Community Guidelines for Animal Care, DL 116/92, application of the European Communities Council Directive (86/609/EEC). Experiments were carried out on rat hippocampal slices, prepared as previously described.<sup>71</sup> Male Wistar rats (Harlan Italy; Udine Italy, 150–200 g body weight) were killed with a guillotine under anesthesia with ether and their hippocampi were rapidly removed and placed in ice-cold oxygenated (95% O<sub>2</sub>–5% CO<sub>2</sub>) aCSF of the following composition (mM): NaCl 124, KCl 3.33, KH<sub>2</sub>PO<sub>4</sub> 1.25, MgSO<sub>4</sub> 1.4, CaCl<sub>2</sub> 2.5, NaHCO<sub>3</sub> 25, and D-glucose 10. Slices (400 μm thick) were cut using a McIlwain tissue chopper (The Mickle Lab. Engineering, Co. Ltd, Gomshall, UK) and kept in oxygenated aCSF for at least 1 h at room temperature. A single slice was then placed on a nylon mesh, completely submerged in a small chamber (0.8 mL), and superfused with oxygenated aCSF (30–32 °C) at a constant flow rate of 1.5/2 mL min<sup>-1</sup>. The treated solutions reached the preparation in 90 s and this delay was taken into account in our calculations.

**6.3.7.1. Extracellular recording.** Test pulses (80 μs, 0.066 Hz) were delivered through a bipolar nichrome electrode positioned in the stratum radiatum. Evoked extracellular potentials were recorded with glass microelectrodes (2–10 MΩ, Clark Electromedical Instruments, Pangbourne, UK) filled with 150 mM NaCl, placed in the CA1 region of the stratum radiatum. Responses

were amplified (BM 622, Mangoni, Pisa, Italy), digitized (sample rate, 33.33 kHz), and stored for later analysis using LTP (version 2.30D) software facilities.<sup>72</sup> Stimulus–response curves were obtained by gradual increases in stimulus strength at the beginning of each experiment, until a stable baseline of evoked response was reached. The test stimulus pulse was then adjusted to produce a fEPSP whose slope and amplitude were 40–50% of the maximum and were kept constant throughout the experiment. The fEPSP amplitude was routinely measured and expressed as the percentage of the average amplitude of the potentials measured during the 5-min preceding exposure of the hippocampal slices to OGD.

In all hippocampal slices, simultaneously with fEPSP amplitude, we also recorded AD in d.c. (direct current) mode and measured from the beginning of OGD as negative d.c. shifts.

**6.3.7.2. Application of drugs and OGD.** OGD was obtained by perfusing the slice for 7 min with aCSF without glucose and gassed with nitrogen (95% N<sub>2</sub>–5% CO<sub>2</sub>).<sup>73</sup> When slices were subjected to 7 min of OGD, if the recovery of fEPSP amplitude after 15 min of reperfusion with glucose-containing and normally oxygenated aCSF was ≤15% of the pre-ischemic value, a second slice from the same rat was submitted to a 7-min OGD insult in the presence of compound **13**. To confirm the result obtained in the treated group, a third slice was taken from the same rat and another 7-min OGD was performed in control conditions, to verify that no difference between slices was caused by the time gap between the experiments.

The selective A<sub>3</sub> adenosine receptor antagonist was applied 15 min before, during, and 5 min after OGD. Concentration of the selective adenosine A<sub>3</sub> receptor antagonist was chosen on the basis of K<sub>i</sub> values on hA<sub>3</sub> AR.

**6.3.7.3. Statistical analysis.** Data were analyzed using Prism 3.02 software (Graphpad Software, San Diego, CA, USA). All numerical data are expressed as means ± SEM. Data were tested for statistical significance by unpaired two-tailed Student's *t* test. A value of *P* < 0.05 was considered significant.

### Acknowledgments

This work was supported by a grant of the Italian Ministry for University and Research (MIUR, FIRB RBNE03YA3L project). The molecular modeling work coordinated by S.M. was carried out with financial support from the University of Padova, Italy, and the Italian Ministry for University and Research (MIUR), Rome, Italy. The electrophysiological work was supported by a grant from the Italian Ministry for University and Research (MIUR) and by Ente Cassa di Risparmio di Firenze (2004/0747). We thank Dr. Karl-Norbert Klotz of the University of Würzburg, Germany, for providing cloned hA<sub>1</sub>, hA<sub>2A</sub>, hA<sub>2B</sub> and hA<sub>3</sub> receptors expressed in CHO cells. S.M. is also very grateful

to Chemical Computing Group for the scientific and technical partnership.

### References and notes

1. Fredholm, B. B.; IJzerman, A. P.; Jacobson, K. A.; Klotz, K. N.; Linden, J. *Pharmacol. Rev.* **2001**, *53*, 527.
2. Jacobson, K. A.; Knutsen, L. J. S. In *Purinergic and Pyrimidinergic Signalling*; Abbracchio, M. P., Williams, M., Eds.; Handbook of Experimental Pharmacology: Berlin, 2001; Vol. 151/1, p 129.
3. Abbracchio, M. P.; Brambilla, R.; Kim, H. O.; von Lubitz, D. K. J. E.; Jacobson, K. A.; Cattabeni, F. *Mol. Pharmacol.* **1995**, *48*, 1083.
4. Ali, H.; Choi, O. H.; Fraundorfer, P. F.; Yamada, K.; Gonzaga, H. M. S.; Beaven, M. A. *J. Pharmacol. Exp. Ther.* **1996**, *276*, 837.
5. Shneyvays, V.; Leshem, D.; Zinman, T.; Mamedova, L. K.; Jacobson, K. A.; Shainberg, A. *Am. J. Physiol. Heart Circ. Physiol.* **2005**, *288*, H2792.
6. Linden, J. *Trends Pharmacol. Sci.* **1994**, *15*, 298.
7. Liang, B. T.; Jacobson, K. A. *Proc. Natl. Acad. Sci. U.S.A.* **1998**, *95*, 6995.
8. Young, H. W.; Molina, J. G.; Dimina, D.; Zhong, H.; Jacobson, M.; Chan, L. N.; Chan, L.-N. L.; Chan, T.-S.; Lee, J. J.; Blackburn, M. R. *J. Immunol.* **2004**, *173*, 1380.
9. Merighi, S.; Mirandola, P.; Varani, K.; Gessi, S.; Leung, E.; Baraldi, P. G.; Tabrizi, M. A.; Borea, P. A. *Pharmacol. Ther.* **2003**, *100*, 31.
10. Jacobson, K. A.; Gao, Z.-G. *Nat. Rev. Drug Disc.* **2006**, *5*, 247.
11. Lee, H. T.; Ota-Setlik, A.; Xu, H.; D'Agati, V. D.; Jacobson, M. A.; Emala, C. W. *Am. J. Physiol. Renal Physiol.* **2003**, *284*, 267.
12. Brambilla, R.; Cattabeni, F.; Ceruti, S.; Barbieri, D.; Franceschi, C.; Kim, Y.-C.; Jacobson, K. A.; Klotz, K.-N.; Lohse, M. J.; Abbracchio, M. P. *Naunyn-Schmiedeberg's Arch. Pharmacol.* **2000**, *361*, 225.
13. Pugliese, A. M.; Coppi, E.; Spalluto, G.; Corradetti, R.; Pedata, F. *Br. J. Pharmacol.* **2006**, *147*, 524.
14. Merighi, S.; Benini, A.; Mirandola, P.; Gessi, S.; Varani, K.; Leung, E.; MacLennan, S.; Borea, P. A. *Biochem. Pharmacol.* **2006**, *72*, 19.
15. Colotta, V.; Catarzi, D.; Varano, F.; Cecchi, L.; Filacchioni, G.; Martini, C.; Trincavelli, L.; Lucacchini, A. *J. Med. Chem.* **2000**, *43*, 3118.
16. Colotta, V.; Catarzi, D.; Varano, F.; Cecchi, L.; Filacchioni, G.; Martini, C.; Trincavelli, L.; Lucacchini, A. *J. Med. Chem.* **2000**, *43*, 1158.
17. Colotta, V.; Catarzi, D.; Varano, F.; Filacchioni, G.; Martini, C.; Trincavelli, L.; Lucacchini, A. *Bioorg. Med. Chem.* **2003**, *11*, 3541.
18. Colotta, V.; Catarzi, D.; Varano, F.; Filacchioni, G.; Martini, C.; Trincavelli, L.; Lucacchini, A. *Bioorg. Med. Chem.* **2003**, *11*, 5509.
19. Colotta, V.; Catarzi, D.; Varano, F.; Calabri, F. R.; Lenzi, O.; Filacchioni, G.; Trincavelli, L.; Martini, C.; Deflorian, F.; Moro, S. *J. Med. Chem.* **2004**, *47*, 3580.
20. Catarzi, D.; Colotta, V.; Varano, F.; Calabri, F. R.; Lenzi, O.; Filacchioni, G.; Trincavelli, L.; Martini, C.; Tralli, A.; Montopoli, C.; Moro, S. *Bioorg. Med. Chem.* **2005**, *13*, 705.
21. Catarzi, D.; Colotta, V.; Varano, F.; Lenzi, O.; Filacchioni, G.; Trincavelli, L.; Martini, C.; Montopoli, C.; Moro, S. *J. Med. Chem.* **2005**, *48*, 7932.
22. Lenzi, O.; Colotta, V.; Catarzi, D.; Varano, F.; Filacchioni, G.; Martini, C.; Trincavelli, L.; Ciampi, O.; Mari-

- ghetti, F.; Morizzo, E.; Moro, S. *J. Med. Chem.* **2006**, *49*, 3916.
23. Colotta, V.; Catarzi, D.; Varano, F.; Capelli, F.; Lenzi, O.; Filacchioni, G.; Martini, C.; Trincavelli, L.; Ciampi, O.; Pugliese, A. M.; Pedata, F.; Schiesaro, A.; Morizzo, E.; Moro, S. *J. Med. Chem.* **2007**, *50*, 40.
24. Chang, L. C. W.; Brussee, J.; IJzerman, A. P. *Chem. Biodivers.* **2004**, *1*, 1591.
25. Ukena, D.; Jacobson, K. A.; Padgett, W. L.; Ayala, C.; Shamim, M. T.; Kirk, K. L.; Olsson, R. O.; Daly, J. W. *FEBS Lett.* **1986**, *209*, 122.
26. Muller, C. *Exp. Opin. Ther. Patents* **1997**, *7*, 419.
27. Moro, S.; Deflorian, F.; Spalluto, G.; Pastorin, G.; Cacciari, B.; Kim, S.-K.; Jacobson, K. A. *Chem. Commun. (Camb.)* **2003**, *24*, 2949.
28. Moro, S.; Spalluto, G.; Jacobson, K. A. *Trends Pharmacol. Sci.* **2005**, *26*, 44.
29. Moro, S.; Deflorian, F.; Bacilieri, M.; Spalluto, G. *Curr. Med. Chem.* **2006**, *13*, 639.
30. Moro, S.; Bacilieri, M.; Deflorian, F.; Spalluto, G. *New J. Chem.* **2006**, *30*, 301.
31. Moro, S.; Deflorian, F.; Bacilieri, M.; Spalluto, G. *Curr. Pharm. Des.* **2006**, *12*, 2175.
32. Tafi, A.; Bernardini, C.; Botta, M.; Corelli, F.; Andreini, M.; Martinelli, A.; Ortore, G.; Baraldi, P. G.; Fruttarolo, F.; Borea, P. A.; Tuccinardi, T. *J. Med. Chem.* **2006**, *49*, 4085.
33. Kim, S. K.; Gao, Z. G.; Jeong, L. S.; Jacobson, K. A. *J. Mol. Graphics Modell.* **2006**, *25*, 562.
34. Jiang, Q.; Lee, B. X.; Glashofer, M.; van Rhee, A. M.; Jacobson, K. A. *J. Med. Chem.* **1997**, *40*, 2588.
35. Jiang, Q.; Van Rhee, A. M.; Kim, J.; Yehle, S.; Wess, J., et al. *Mol. Pharmacol.* **1996**, *50*, 512.
36. Latini, S.; Pedata, F. *J. Neurochem.* **2001**, *79*, 463.
37. Pugliese, A. M.; Coppi, E.; Volpini, R.; Cristalli, G.; Corradetti, R.; Jeong, L. S.; Jacobson, K. A.; Pedata, F. *Biochem. Pharmacol.* **2007**, *74*, 768.
38. Obeidat, A. S.; Andrew, R. D. *Eur. J. Neurosci.* **1998**, *10*, 3451.
39. Somjen, G. G. *Physiol. Rev.* **2001**, *81*, 1065.
40. Latini, S.; Bordoni, F.; Pedata, F.; Corradetti, R. *Br. J. Pharmacol.* **1999**, *127*, 729.
41. Pearson, T.; Damian, K.; Lynas, R. E.; Frenguelli, B. G. *J. Neurochem.* **2006**, *97*, 1357.
42. Jeong, L. S.; Choe, S. A.; Gunaga, P.; Kim, H. O.; Lee, H. W.; Lee, S. K.; Tosh, D.; Patel, A.; Palaniappan, K. K.; Gao, Z. G.; Jacobson, K. A.; Moon, H. R. *J. Med. Chem.* **2007**, *50*, 3159.
43. Li, A.-H.; Moro, S.; Melman, N.; Ji, X.-d.; Jacobson, K. A. *J. Med. Chem.* **1998**, *41*, 3186.
44. Kim, Y.-C.; Ji, X.-d.; Jacobson, K. A. *J. Med. Chem.* **1996**, *39*, 4142.
45. Maconi, A.; Pastorin, G.; da Ros, T.; Spalluto, G.; Gao, Z.-G.; Jacobson, K. A.; Baraldi, P. G.; Cacciari, B.; Varani, K.; Moro, S.; Borea, P. A. *J. Med. Chem.* **2002**, *45*, 3579.
46. Ji, X. D.; Gallo-Rodriguez, C.; Jacobson, K. A. *Biochem. Biophys. Res. Commun.* **1994**, *203*, 570.
47. von Lubitz, D. K. *Eu. J. Pharmacol.* **1999**, *263*, 59.
48. Tanaka, E.; Yamamoto, S.; Kudo, Y.; Mihara, S.; Higashi, H. *J. Neurophysiol.* **1997**, *78*, 891.
49. Yamamoto, S.; Tanaka, E.; Shoji, Y.; Kudo, Y.; Inokuchi, H.; Higashi, H. *J. Neurophysiol.* **1997**, *78*, 903.
50. Nieber, K.; Hentschel, S. In *Proceedings of the 8th International Symposium on Adenosine and Adenine Nucleotides*, Ferrara, Italy, May 24–28, 2006.
51. Macek, T. A.; Schaffhauser, H.; Conn, P. J. *J. Neurosci.* **1998**, *18*, 6138.
52. Yli-Kauhahuoma, J. T.; Ashkey, J. A.; Lo, C.-H.; Toker, L.; Wolfe, M. M.; Janda, K. D. *J. Am. Chem. Soc.* **1995**, *117*, 7041.
53. Yu, D.-W.; Gatley, S. J.; Wolf, A. P.; MacGregor, R. R.; Dewey, S. L.; Fowler, J. S.; Schlyer, D. J. *J. Med. Chem.* **1992**, *35*, 2178.
54. Schnetteler, R. A.; Dage, R. C.; Palopoli, F. P. *J. Med. Chem.* **1986**, *29*, 860.
55. OpenMosix: <http://www.openMosix.org>, 2004.
56. MOE (The Molecular Operating Environment) Version 2006.08, software available from Chemical Computing Group Inc., 1010 Sherbrooke Street West, Suite 910, Montreal, Canada H3A 2R7. <http://www.chemcomp.com>.
57. MOPAC 7, J.J.P. Stewart, Fujitsu Limited, Tokyo, Japan, 1993.
58. Palczewski, K.; Kumasaka, T.; Hori, T.; Behnke, C. A.; Motoshima, H., et al. *Science* **2000**, *289*, 739.
59. Cornell, W. D. C. P.; Bayly, C. I.; Gould, I. R.; Merz, K. M.; Ferguson, D. M.; Spellmeyer, D. C.; Fox, T.; Caldwell, J. W.; Kollman, P. A. *J. Am. Chem. Soc.* **1995**, *117*, 5179.
60. Levitt, M. *J. Mol. Biol.* **1992**, *226*, 507.
61. Baxter, C. A.; Murray, C. W.; Clark, D. E.; Westhead, D. R.; Eldridge, M. D. *Funct. Genet.* **1998**, *33*, 367.
62. Halgren, T. *J. Comput. Chem.* **1996**, *17*, 490.
63. Manetti, F.; Schenone, S.; Bondavalli, F.; Brullo, C.; Bruno, O.; Ranise, A.; Mosti, L.; Menozzi, G.; Fossa, P.; Trincavelli, M. L.; Martini, C.; Martinelli, A.; Tintori, C.; Botta, M. *J. Med. Chem.* **2005**, *48*, 7172.
64. Colotta, V.; Catarzi, D.; Varano, F.; Melani, F.; Filacchioni, G.; Cecchi, L.; Trincavelli, L.; Martini, C.; Lucacchini, A. *Farmacol.* **1998**, *53*, 189.
65. Novellino, E.; Cosimelli, B.; Ehlaro, M.; Greco, G.; Iadanza, M.; Lavecchia, A.; Rimoli, M. G.; Sala, A.; Da Settimo, A.; Primofiore, G.; Da Settimo, F.; Taliani, S.; La Motta, C.; Klotz, K.-N.; Tuscano, D.; Trincavelli, M. L.; Martini, C. *J. Med. Chem.* **2005**, *48*, 8253.
66. Klotz, K.-N.; Vogt, H.; Tawfik-Schlieper, H. *Naunyn-Schmiedeberg's Arch Pharmacol.* **1991**, *343*, 196.
67. Mazzoni, M. R.; Buffoni, R. S.; Giusti, L.; Lucacchini, A. *J. Recept. Signal Transduct. Res.* **1995**, *15*, 905.
68. Nordstedt, C.; Fredholm, B. *Anal. Biochem.* **1990**, *189*, 231.
69. Cheng, Y. C.; Prusoff, W. H. *Biochem. Pharmacol.* **1973**, *22*, 3099.
70. Pugliese, A. M.; Latini, S.; Corradetti, R.; Pedata, F. *Br. J. Pharmacol.* **2003**, *140*, 305.
71. Anderson, W. W.; Collingridge, G. L. *J. Neurosci. Methods* **2001**, *108*, 7.
72. Pedata, F.; Latini, S.; Pugliese, A. M.; Pepeu, G. *J. Neurochem.* **1993**, *61*, 284.